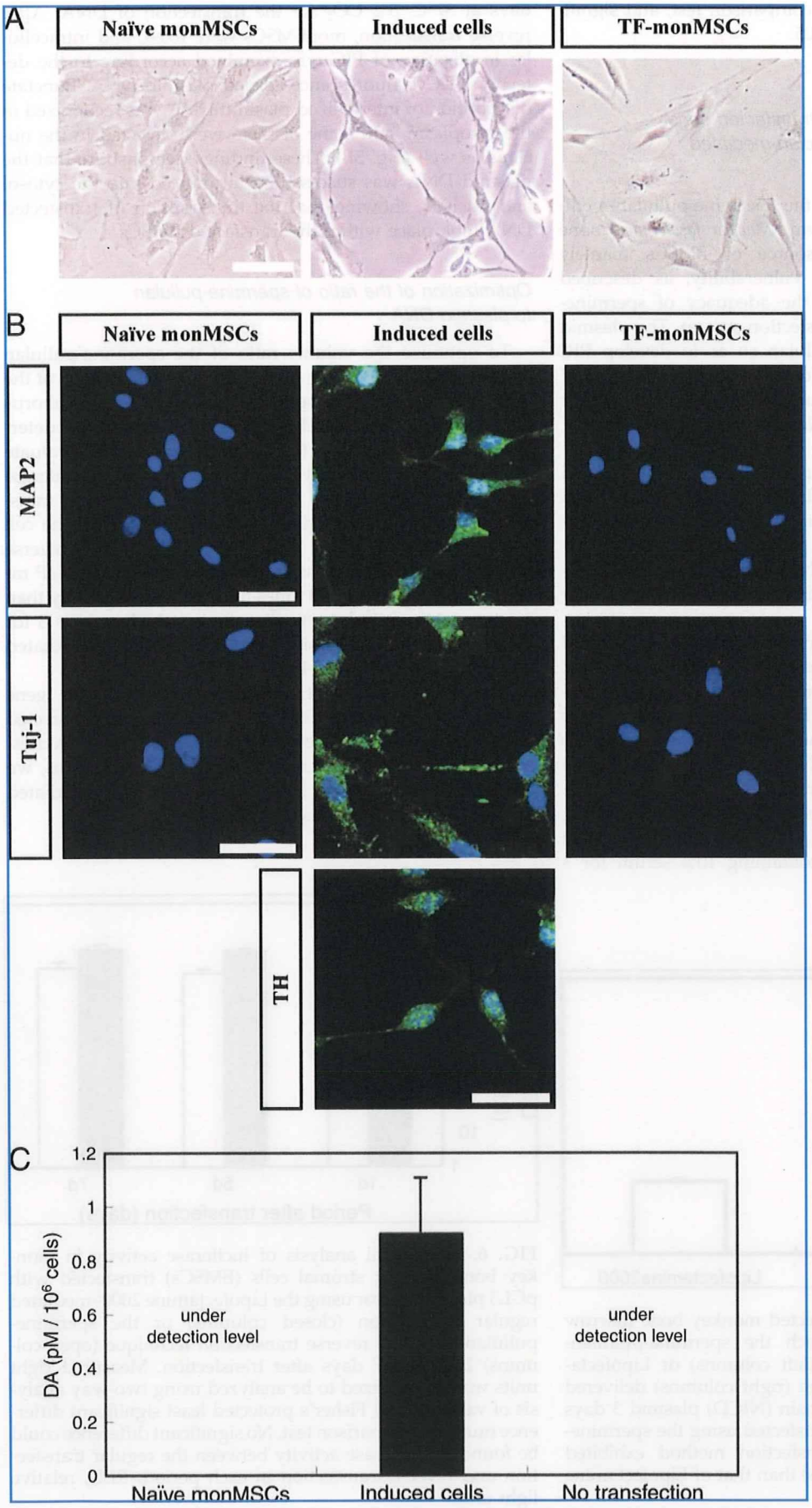

FIG. 7. Morphological and functional characterization of naïve monkey bone marrow stromal cells (monBMSCs) induced neuronal cells and trophic factor–treated monMSCs without the reverse transfection of pCI-Notch intracellular domain (NICD; TF-monMSCs, see text). (**A**) Phase contrast images. Induced neuronal cells exhibited round cell bodies with neurite-like processes. (**B**) Immunocytochemistry for neuronal markers. Induced neuronal cells were positive for neuron-specific antigens microtubule-associated protein (MAP)2 and anti-beta-tubulin class III (Tuj-1). Tyrosine hydroxylase–positive neuronal cells detected after further treatment of induced neuronal cells with glial cell line–derived neurotrophic factor. Most naïve monMSCs and TF-monMSCs were negative to MAP2 and Tuj-1. (**C**) Dopamine release assay detected using high-performance liquid chromatography. Sequential treatment of low and high K^+ condition stimulated the secretion of dopamine. A substantial increase in dopamine secretion was detected only in induced neuronal cells (middle column) but was under detection levels in naïve monMSCs and TF-monMSCs (left and right columns, respectively). Data were collected from three independent experiments. Scale bars: 100 μm.

Low toxicity of spermine-pullulan-mediated transfection

Next, we measured the viability of cells transfected with plasmid DNA. Figure 5 showed that only $31.6 \pm 1.4\%$ of transfected monBMSCs survived after transfection of the pCI-NICD plasmid using 4-h incubation of Lipofectamine 2000 even in the presence of 10% FCS. On the other hand, $97.0 \pm 4.1\%$ of monBMSCs survived after reverse transfection at 3 days. Considering our method for the induction of neuronal cells from BMSCs, where further treatment with G418 selection and trophic factor stimulation is required, the low cytotoxicity of this reverse transfection condition is the great advantage of the gene delivery in our system.

Efficiency of spermine-pullulan-mediated transfection

To test the efficiency of this transfection system, the sequential luciferase assay was performed from day 1 to 7 after starting the reverse transfection. Comparing the luciferase activity of spermine-pullulan-mediated reverse transfection with that of Lipofectamine 2000, there was no statistical difference in their protein expression level from day 1 to 7 (Fig. 6).

Functional assessment of spermine-pullulan-mediated transfection through neuronal cell induction assay from BMSCs

We have estimated the viability and efficiency of this spermine-pullulan-mediated reverse transfection system and found that the viability was much higher than, and the efficiency was as same as, that of Lipofectamine 2000. The efficiency was estimated according to luciferase activity—a functional but simple assay for protein expression. The main objective in this study was to focus on verifying the availability of this reverse transfection system for the induction of neuronal cells (dopamine-producing cells) from various kinds of BMSCs, including monBMSCs. This induction system comprised NICD plasmid transfection, selection of transfected cells by G418, and trophic factor stimulation—much different from simple protein expression such as luciferase activity (Fig. 1). We therefore introduced pCI-NICD plasmid into monBMSCs using spermine-pullulan-mediated reverse transfection. Three days after starting reverse transfection, transfected cells were selected using the G418 treatment for 5 to 7 days, re-plated at a cell density of 2,080 cells/cm^2, and incubated with culture medium (10% FBS in α-MEM) containing bFGF, FSK, and CNTF for 3 days. Naïve monBMSCs exhibited fibroblast-like mesenchymal morphology (naïve monBMSCs; Fig. 7A), as has been reported in BMSCs from other species.[26,27] Cell morphology did not change significantly after the introduction of NICD plasmid, although after treatment with trophic factors, cells exhibited round cell bodies and extended neurite-like processes, which were similar to neuronal cells (induced cells; Fig. 7A). To evaluate whether the gene introduction of NICD is essential for the induction of neuronal cells from BMSCs, monBMSCs treated with three trophic factors without the reverse transfection of pCI-NICD plasmid (TF-monBMSCs, see Materials and Methods) were used. No morphological change was observed in TF-monBMSCs (Fig. 7A), as has been reported using rat and human cells in our previous study.[15] Immunocytochemistry demonstrated that neuron-specific markers MAP2 and Tuj-1 were positive in induced neuronal cells but were not detectable in most naïve monBMSCs (Fig. 7B), suggesting the induction of neuronal cells from monBMSCs. The trophic factor treatment did not increase MAP2 or Tuj-1 expression in monBMSCs (Fig. 7B, TF-monBMSCs). These induced neuronal cells were further treated with GDNF, a trophic factor known to induce dopaminergic neurons in the midbrain during development (Fig. 1).[17] Immunocytochemistry for TH, a marker for dopaminergic neurons, showed positive cells in the GDNF-treated neuronal cells, suggesting the induction of dopaminergic neurons from monBMSCs (Fig. 7B). The most important thing was to confirm whether these induced neuronal cells have an ability to produce and release dopamine. Therefore, we measured the secretion of dopamine by these induced cells using HPLC (Fig. 7C). The dopamine activity in the culture supernatant was measured after induction of dopamine release by high K^+ depolarizing stimuli; induced cells marked 0.906 pM/10^6 cells of dopamine release, whereas dopamine activity of naïve monBMSCs and TF-monBMSCs were undetectable (Fig. 7C). These results were consistent with those reported in rat BMSC-derived dopamine-producing cells in our previous report.[15] These findings demonstrated that the spermine-pullulan-mediated reverse transfection successfully delivered NICD plasmid so as to induce functional dopamine-producing neuronal cells from monBMSCs.

Neuronal induction in BMSCs from other species

The above data suggest the advantage of a spermine-pullulan-mediated reverse transfection system for BMSCs from other animal species as well. We therefore investigated BMSCs from mice and humans. The morphology of mouse naïve BMSCs is similar to that of monkeys; they are flat or sometimes polygonal shape (naïve mouse BMSCs; Fig. 8A), whereas human BMSCs exhibited longer and thinner morphology than monBMSCs (Naïve human BMSCs; Fig. 8C). After NICD introduction and trophic factor treatment, cells with neuronal characteristics could be successfully induced from BMSCs from both species (Fig. 8A, C). Immunocytochemistry showed that neuronal markers MAP2- (data not shown) and Tuj-1-positive (Fig. 8B for mouse BMSCs) cells were detected after trophic factor treatment in the transfected BMSCs in each species. Dopaminergic neurons detected according to their immunoreactivity to TH could be yielded after further treatment with GDNF from BMSCs derived from both species (Fig. 8B for mouse BMSCs). Secretion of dopamine after high K^+ treatment was also tested in HPLC and was detected in BMSC-derived dopaminergic neurons but not in naïve BMSCs from both species as in case of monBMSCs (data not shown).

Discussion

In this study, we demonstrated that the spermine-pullulan-mediated reverse transfection is an effective method for the introduction of plasmid genes even into vulnerable cells with high efficiency and low cytotoxicity. Introduced exogenous plasmid genes were successfully transcribed and expressed as protein in the cytoplasm of BMSCs with the smallest level of cell death. This system was also effective for

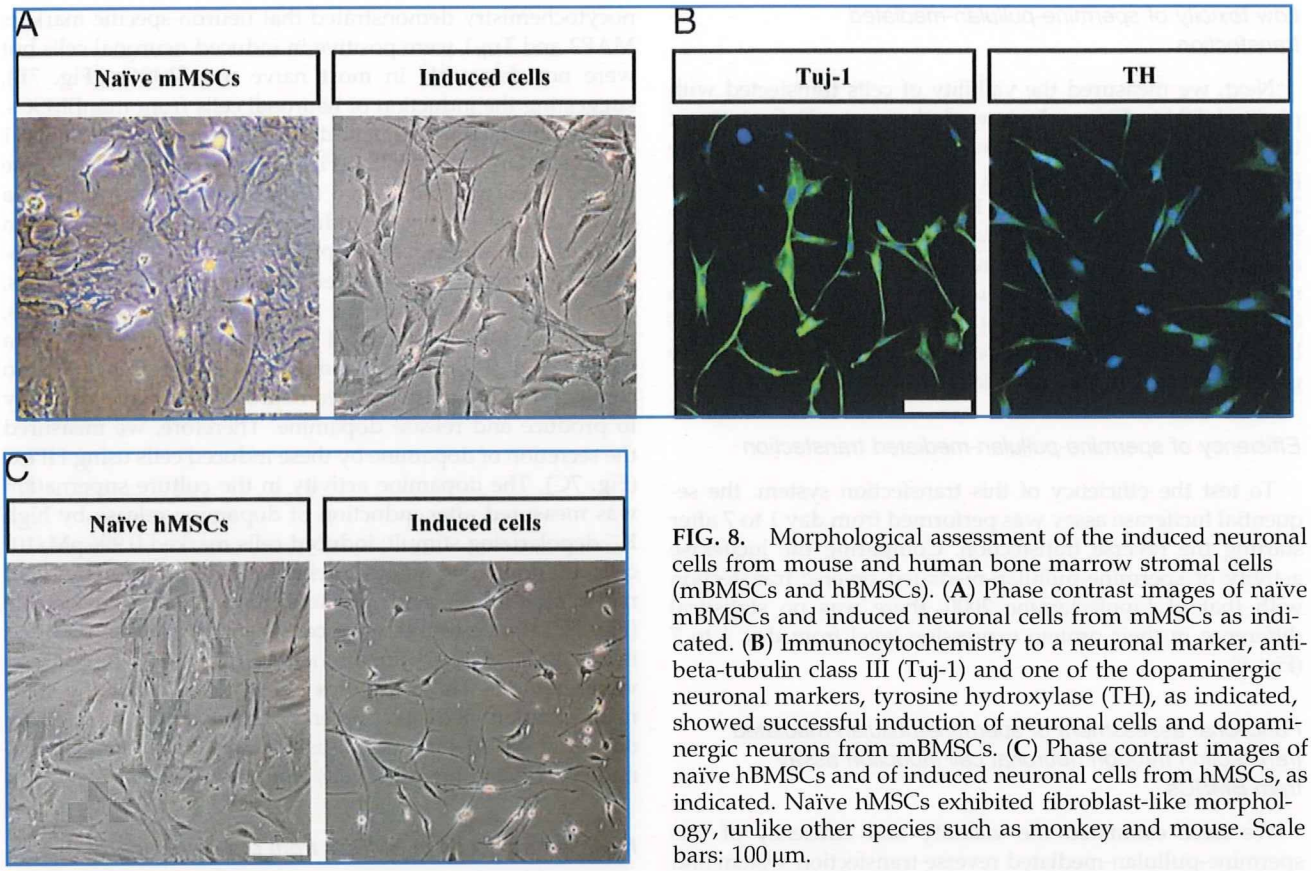

FIG. 8. Morphological assessment of the induced neuronal cells from mouse and human bone marrow stromal cells (mBMSCs and hBMSCs). (**A**) Phase contrast images of naïve mBMSCs and induced neuronal cells from mMSCs as indicated. (**B**) Immunocytochemistry to a neuronal marker, anti-beta-tubulin class III (Tuj-1) and one of the dopaminergic neuronal markers, tyrosine hydroxylase (TH), as indicated, showed successful induction of neuronal cells and dopaminergic neurons from mBMSCs. (**C**) Phase contrast images of naïve hBMSCs and of induced neuronal cells from hMSCs, as indicated. Naïve hMSCs exhibited fibroblast-like morphology, unlike other species such as monkey and mouse. Scale bars: 100 μm.

the induction of dopamine-producing neuronal cells from BMSCs in several kinds of species in which the introduction of NICD plasmid is indispensable for the induction process. This reverse transfection allows transfected cells to survive for further treatment, such as selection by G418. Virtually, sequential treatments comprising reverse transfection, antibiotic selection, and trophic factor stimulation gave the successful induction of mature neuronal cells that have an ability to produce and release dopamine, whose maturation was confirmed using immunocytochemistry and HPLC. Because naïve monBMSCs and TF-monBMSCs did not show neuronal marker expression or dopamine release, it is likely that NICD introduction is required for the effective induction of dopamine-producing cells from BMSCs. These findings also indicated that tangled treatments for induction of specific cells after this spermine-pullulan-mediated reverse transfection can be applied to the multipotent cells to obtain desirable results, which can be attributable to no detrimental effect on differentiation activity. Thus, this reverse transfection method may be suitable to the induction of specific cells for cell therapy from pluri- and multipotent cells.

Control for differentiation and induction of stem cells is an important matter in stem cell biology and regenerative medicine. Genetic manipulations such as gene introduction are key ways to modify the differentiation and function of stem cells.[18,19] In this context, it is necessary to develop a gene delivery system with low cytotoxicity and high efficiency. We showed that this reverse transfection method can be applied to the susceptible cells, to which generally gene transfer is difficult, even with high efficiency. Thus, our data clearly indicate that the spermine-pullulan-mediated reverse transfection is one of the most practical methods of genetically modifying the differentiation of BMSCs, which is also applicable to other kinds of tissue stem cells.

BMSCs offer possibilities for clinical application, because they can be efficiently expanded *in vitro* to achieve a therapeutic scale. They are easily accessible through the aspiration of bone marrow and can easily be expanded on a large scale for auto-transplantation. We can collect BMSCs without encountering serious ethical problems, and there is no need to use a fertilized egg or fetus. Thus, BMSCs are strong and hopeful candidates for use in cell-based therapy. In addition, because BMSCs are obtained from marrow banks, transplantation of induced cells with the same human leukocyte antigen subtype from a healthy donor may minimize the risk of rejection.

Because BMSCs can be obtained from patients, it is possible to establish "auto cell transplantation therapy" using BMSCs. Fortunately, we have confirmed that human serum is more appropriate for the differentiation of human BMSCs than fetal bovine serum (unpublished data). To realize this ideal, it is necessary to develop a practical system of differentiating BMSCs into cells with a purpose. For Parkinson's disease, transplantation of dopaminergic neurons is believed to be effective.[28] Our method would be one possible way to regulate BMSC differentiation into functional dopaminergic neuronal cells, which will be applicable to auto-transplantation therapy in Parkinson's disease.

Taking into account the anchoring of the plasmid DNA on the surface of culture dishes, one possibility is that

this reverse transfection system will be able to control spatially specific gene introduction. This reverse transfection technique may provide two-dimensional or even three-dimensional control of gene expression so that accurate alignment of specific cells can be acquired. In our previous study, we found that high concentration of ProNectin coating on the surface of culture dishes provided more luciferase activity in a dose-dependent manner,[20] indicating that, in addition to changing the promoter of plasmid DNA, the concentration of adhesion substrate can modify the protein expression level. Although application of cell therapy has not been considered adequate for the repair of tissue that is composed of a complex organization of cells, this reverse transfection method might allow the strategy to construct the tissue itself.

As mentioned, five steps are important for gene expression of transfected plasmid DNA, from the first step of attachment on the cell membrane thorough internalization into the nucleus. Cy5-labeled plasmid DNA was detected in the cytosol and nucleus 3 days after reverse transfection, demonstrating internalization of plasmid DNA into the cytoplasm and nucleus. The mechanism of internalization of plasmid DNA into the cytoplasm is considered to be achieved through sugar-recognizable receptors, but the mechanisms of traverse in the cytosol and internalization into the cell nucleus are still unknown. It has been hypothesized that the plasmid DNA delivered by this reverse transfection incorporates into the nucleus when the nuclear pore disappears during cell division, as is the case with regular transfection, which is different from virus-mediated gene transfer. Our induction method for neuronal cells from BMSCs does not need sequential gene manipulation, so this point is not problematic in our system. For application of this reverse transfection method to induce the specific cell under the specific condition, we must be aware of the possibility that functional gene expression transfected using this reverse transfection technique will not be achieved after cells are post-mitotic, even when plasmid DNA is internalized into the cytoplasm.

The plasmid DNA intermingled with spermine-pullulan (PIC) could be easily fixed on the surface of Pronectin- and gelatin-coated culture dishes. For spermine-pullulan-mediated reverse transfection, cells were seeded on the culture dishes fixed with PIC and incubated for 24 h after seeding. Plasmid DNA could penetrate into the cell membrane and the nucleus at 3 days after reverse transfection. Almost all transfected cells survived after transfection, and the expression intensity of exogenous gene was determined using luciferase assay, which showed almost the same level of protein expression as that of Lipofectamine 2000. For this low toxicity, monBMSCs, which are vulnerable to manipulation such as gene introduction and reagent stimulation, were used in our study for dopaminergic neuronal cell induction. Cells were introduced with NICD, selected with G418, and followed using trophic factor treatment. Morphological and immunocytochemical analysis showed the induction of neuronal cells from monBMSCs. Additional GDNF treatment promoted BMSC-derived neuronal cells to dopamine-producing cells; immunocytochemistry showed the expression of dopaminergic neuron marker TH and the secretion of dopamine detected using HPLC. BMSCs derived from mice and humans also demonstrated basically identical results to those of monBMSCs. These results showed that the spermine-pullulan-mediated reverse transfection technique is effective in functional dopaminergic neuronal cell-induction from several kinds of BMSCs that will be applicable to genetic manipulation of stem cells.

Acknowledgments

This study was supported by the Ministry of Health, Labor and Welfare (Research on Psychiatric and Neurological Diseases and Mental Health) and the Program for Promotion of Fundamental Studies in Health Sciences of the National Institute of Biomedical Innovation.

Disclosure Statement

No competing financial interests exist.

References

1. De Bari C, Dell'Accio F, Vandenabeele F, Vermeesch JR, Raymackers JM, Luyten FP. Skeletal muscle repair by adult human mesenchymal stem cells from synovial membrane. J Cell Biol. **160,** 909, 2003.
2. Makino S, Fukuda K, Miyoshi S, Konishi F, Kodama H, Pan J, Sano M, Takahashi T, Hori S, Abe H, Hata J, Umezawa A, Ogawa S. Cardiomyocytes can be generated from marrow stromal cells in vitro. J Clin Invest. **103,** 697, 1999.
3. McBeath R, Pirone DM, Nelson CM, Bhadriraju K, Chen CS. Cell shape, cytoskeletal tension, and RhoA regulate stem cell lineage commitment. Dev Cell. **6,** 483, 2004.
4. Mezey E, Chandross KJ, Harta G, Maki RA, McKercher SR. Turning blood into brain: cells bearing neuronal antigens generated in vivo from bone marrow. Science. **290,** 1779, 2000.
5. Muguruma Y, Yahata T, Miyatake H, Sato T, Uno T, Itoh J, Kato S, Ito M, Hotta T, Ando K. Reconstitution of the functional human hematopoietic microenvironment derived from human mesenchymal stem cells in the murine bone marrow compartment. Blood. **107,** 1878, 2006.
6. Pittenger MF, Mackay AM, Beck SC, Jaiswal RK, Douglas R, Mosca JD, Moorman MA, Simonetti DW, Craig S, Marshak DR. Multilineage potential of adult human mesenchymal stem cells. Science. **284,** 143, 1999.
7. Prockop DJ. Marrow stromal cells as stem cells for nonhematopoietic tissues. Science. **276,** 71, 1997.
8. Prockop DJ. Further proof of the plasticity of adult stem cells and their role in tissue repair. J Cell Biol. **160,** 807, 2003.
9. Rafii S, Lyden D. Therapeutic stem and progenitor cell transplantation for organ vascularization and regeneration. Nat Med. **9,** 702, 2003.
10. Sato Y, Araki H, Kato J, Nakamura K, Kawano Y, Kobune M, Sato T, Miyanishi K, Takayama T, Takahashi M, Takimoto R, Iyama S, Matsunaga T, Ohtani S, Matsuura A, Hamada H, Niitsu Y. Human mesenchymal stem cells xenografted directly to rat liver are differentiated into human hepatocytes without fusion. Blood. **106,** 756, 2005.
11. Werner N, Junk S, Laufs U, Link A, Walenta K, Bohm M, Nickenig G. Intravenous transfusion of endothelial progenitor cells reduces neointima formation after vascular injury. Circ Res. **93,** e17, 2003.
12. Dezawa M. Insights into autotransplantation: the unexpected discovery of specific induction systems in bone marrow stromal cells. Cell Mol Life Sci. **63,** 2764, 2006.

13. Kawate K, Yajima H, Ohgushi H, Kotobuki N, Sugimoto K, Ohmura T, Kobata Y, Shigematsu K, Kawamura K, Tamai K, Takakura Y. Tissue-engineered approach for the treatment of steroid-induced osteonecrosis of the femoral head: transplantation of autologous mesenchymal stem cells cultured with beta-tricalcium phosphate ceramics and free vascularized fibula. Artif Organs. **30,** 960, 2006.
14. Dezawa M, Ishikawa H, Itokazu Y, Yoshihara T, Hoshino M, Takeda S, Ide C, Nabeshima Y. Bone marrow stromal cells generate muscle cells and repair muscle degeneration. Science. **309,** 314, 2005.
15. Dezawa M, Kanno H, Hoshino M, Cho H, Matsumoto N, Itokazu Y, Tajima N, Yamada H, Sawada H, Ishikawa H, Mimura T, Kitada M, Suzuki Y, Ide C. Specific induction of neuronal cells from bone marrow stromal cells and application for autologous transplantation. J Clin Invest. **113,** 1701, 2004.
16. Mimura T, Dezawa M, Kanno H, Yamamoto I. Behavioral and histological evaluation of a focal cerebral infarction rat model transplanted with neurons induced from bone marrow stromal cells. J Neuropathol Exp Neurol. **64,** 1108, 2005.
17. Akerud P, Alberch J, Eketjall S, Wagner J, Arenas E. Differential effects of glial cell line-derived neurotrophic factor and neurturin on developing and adult substantia nigra dopaminergic neurons. J Neurochem. **73,** 70, 1999.
18. Mangi AA, Noiseux N, Kong D, He H, Rezvani M, Ingwall JS, Dzau VJ. Mesenchymal stem cells modified with Akt prevent remodeling and restore performance of infarcted hearts. Nat Med. **9,** 1195, 2003.
19. Yokoo T, Ohashi T, Shen JS, Sakurai K, Miyazaki Y, Utsunomiya Y, Takahashi M, Terada Y, Eto Y, Kawamura T, Osumi N, Hosoya T. Human mesenchymal stem cells in rodent whole-embryo culture are reprogrammed to contribute to kidney tissues. Proc Natl Acad Sci U S A. **102,** 3296, 2005.
20. Okazaki A, Jo J, Tabata Y. A reverse transfection technology to genetically engineer adult stem cells. Tissue Eng. **13,** 245, 2007.
21. Hermanson GT. Bioconjugate Techniques, San Diego, CA: Academic Press; 1996.
22. Yamamoto N, Yamamoto S, Inagaki F, Kawaichi M, Fukamizu A, Kishi N, Matsuno K, Nakamura K, Weinmaster G, Okano H, Nakafuku M. Role of Deltex-1 as a transcriptional regulator downstream of the Notch receptor. J Biol Chem. **276,** 45031, 2001.
23. Dezawa M, Takahashi I, Esaki M, Takano M, Sawada H. Sciatic nerve regeneration in rats induced by transplantation of in vitro differentiated bone-marrow stromal cells. The European journal of neuroscience. **14,** 1771, 2001.
24. Habeeb AF. Determination of free amino groups in proteins by trinitrobenzenesulfonic acid. Anal Biochem. **14,** 328, 1966.
25. Nagano Y, Yamashita H, Takahashi T, Kishida S, Nakamura T, Iseki E, Hattori N, Mizuno Y, Kikuchi A, Matsumoto M. Siah-1 facilitates ubiquitination and degradation of synphilin-1. J Biol Chem. **278,** 51504, 2003.
26. Kopen GC, Prockop DJ, Phinney DG. Marrow stromal cells migrate throughout forebrain and cerebellum, and they differentiate into astrocytes after injection into neonatal mouse brains. Proc Natl Acad Sci U S A. **96,** 10711, 1999.
27. Shimizu S, Kitada M, Ishikawa H, Itokazu Y, Wakao S, Dezawa M. Peripheral nerve regeneration by the in vitro differentiated-human bone marrow stromal cells with Schwann cell property. Biochem Biophys Res Commun. **359,** 915, 2007.
28. Kawasaki H, Mizuseki K, Nishikawa S, Kaneko S, Kuwana Y, Nakanishi S, Nishikawa SI, Sasai Y. Induction of midbrain dopaminergic neurons from ES cells by stromal cell-derived inducing activity. Neuron. **28,** 31, 2000.

Address reprint requests to:
Mari Dezawa, M.D., Ph.D.
Department of Stem Cell Biology and Histology
Tohoku University Graduate School of Medicine
2-1 Seiryo-machi, Aoba-ku, Sendai 980-8575
Japan

E-mail: mdezawa@m.tains.tohoku.ac.jp

Received: August 8, 2008
Accepted: October 15, 2008
Online Publication Date: January 16, 2009

Journal of Cerebral Blood Flow & Metabolism (2009) 29, 1409–1420

www.jcbfm.com

Committed neural progenitor cells derived from genetically modified bone marrow stromal cells ameliorate deficits in a rat model of stroke

Makoto Hayase[1], Masaaki Kitada[2,3], Shohei Wakao[2,3], Yutaka Itokazu[2], Kazuhiko Nozaki[1,4], Nobuo Hashimoto[1,5], Yasushi Takagi[1] and Mari Dezawa[2,3]

[1]*Department of Neurosurgery, Kyoto University Graduate School of Medicine, 54 Kawahara-cho, Shogoin, Sakyo-ku, Kyoto, Japan;* [2]*Department of Anatomy and Neurobiology, Kyoto University Graduate School of Medicine, Yoshidakonoe-cho, Sakyo-ku, Kyoto, Japan;* [3]*Department of Stem Cell Biology and Histology, Tohoku University Graduate School of Medicine, 2-1, Seiryo-machi, Aoba-ku, Sendai, Japan;* [4]*Department of Neurosurgery, Shiga University of Medical Science, Seta Tsukinowa-cho, Otsu City, Shiga, Japan;* [5]*National Cardiovascular Center, 5-7-1, Fujishiro-dai, Suita City, Osaka, Japan*

Bone marrow stromal cells (MSCs) are an excellent source of cells for treating a variety of central nervous system diseases. In this study, we report the efficient induction of committed neural progenitor cells from rat and human MSCs (NS-MSCs) by introduction of cells with the intracellular domain of Notch-1 followed by growth in the free-floating culture system. NS-MSCs successfully formed spheres, in which cells highly expressed the neural precursor cell markers. The commitment of spheres to neural lineage cells was confirmed by their successful differentiation into neuronal cells when exposed to a differentiation medium. To determine the therapeutic potential of NS-MSCs, cells were transplanted into the cortex and striatum in a rat model of focal cerebral ischemia. The survival, distribution, and integration of NS-MSCs in the host brain were very high, and at day 100, grafted NS-MSCs were positive for dopaminergic, glutamatergic, and γ-amino butyric acid (GABA)ergic neuronal markers. They extended long neurites for nearly 6.3 mm and many of these expressed synaptophysin. Significant behavioral recovery was also observed in limb-placing and water-maze tests. These suggest a high potential for this MSC approach in the replenishment of neural cells for stroke and for a wide range of neurodegenerative conditions that require various types of neural cells.
Journal of Cerebral Blood Flow & Metabolism (2009) **29,** 1409–1420; doi:10.1038/jcbfm.2009.62; published online 13 May 2009

Keywords: bone marrow stromal cells; cell therapy; cerebral ischemia; neuroprogenitors; neurospheres; transplantation

Correspondence: Dr Y Takagi, Department of Neurosurgery, Kyoto University Graduate School of Medicine, 54 Kawahara-cho, Shogoin, Sakyo-ku, Kyoto, 606-8507 Japan.
E-mail: ytakagi@kuhp.kyoto-u.ac.jp or
Dr M Dezawa, Department of Stem Cell Biology and Histology, Tohoku University Graduate School of Medicine, 2-1 Seiryo-machi, Aoba-ku, Sendai 980-8575, Japan.
E-mail: mdezawa@m.tains.tohoku.ac.jp
This study was supported by the Program for Promotion of Fundamental Studies in Health Sciences of the National Institute of Biomedical Innovation (NIBIO, 05-6) and by the Health and Labor Sciences Research Grants of 'Research on Psychiatric and Neurological Diseases and Mental Health' from the Ministry of Health, Labor and Welfare. This study was also supported by the Grant-in-Aid for Scientific Research (B) (19390074) from the Ministry of Education, Culture, Sports, Science and Technology, Japan.
Received 11 November 2008; revised 24 March 2009; accepted 27 April 2009; published online 13 May 2009

Introduction

Stroke is a major cause of death, followed closely by cancer and myocardial infarction, and is characterized by progressive neurologic deficits. Effective treatments for restoring lost neurologic function are currently lacking (Bliss *et al*, 2007; Lindvall and Kokaia, 2006). Cell transplantation is one potential strategy for the treatment of stroke and other progressive neurodegenerative diseases, such as Parkinson's disease, Alzheimer's disease, and others. Embryonic stem cells (ESCs) and neural stem cells (NSCs) have prompted great interest because of their potential to replenish lost neuronal cells (Reubinoff *et al*, 2001). Stem and/or neural progenitor cells derived from the umbilical cord blood, amnion/placenta, and adipose tissues are also candidates for

cell transplantation therapy (Borlongan *et al*, 2004; Igura *et al*, 2004; In 't Anker *et al*, 2003; Lin *et al*, 2006).

Bone marrow contains mesenchymal stem cells, also known as bone marrow stromal cells (MSCs) that possess the potential to differentiate into other cell types (Prockop, 1997; Tang *et al*, 2007). MSCs are promising candidates for clinical application because they are easily isolated from patient bone marrow aspirates and are readily expanded *in vitro* for auto-transplantation without posing major ethical problems (Dezawa *et al*, 2005). Naive MSCs have been reported by several groups to enhance functional recovery after stroke, with the mechanism of action postulated to be mediated by the trophic effects of MSCs rather than by the spontaneous neuronal differentiation of MSCs in the host brain (Chen *et al*, 2001*a*, *b*; Chen and Chopp, 2006; Li *et al*, 2000, 2002; Shen *et al*, 2007).

In the acute stage of brain injury, neuroprotective treatment may effectively prevent the progressive loss of damaged neuronal cells, but in advanced degenerative stages, neuronal replacement is deemed necessary for cell therapy to exert its benefits. We reported earlier that functional dopaminergic neurons can be specifically induced from human MSCs with a very high efficiency without glial development by the Notch intracellular domain (NICD) transfection followed by the administration of a certain combination of trophic factors, including glial cell line-derived neurotrophic factor (CDNF) (PeproTech, Inc., Rocky Hill, NJ, USA) (Dezawa *et al*, 2004; Mimura *et al*, 2005).

In this study, we newly found that rat and human MSCs shift to a neural progenitor-like state, alternatively, committed neural precursor cells, after receiving Notch signal followed by the culture in the free-floating system. Notch intracellular domain-transfected MSCs (NICD-MSCs) successfully formed spheres (NS-MSCs) that highly expressed neural precursor cell markers. The commitment of spheres to neural lineage cells was further evaluated *in vitro*, which showed that sphere-derived cells successfully differentiated into neuronal cells when exposed to a differentiation medium, and expressed neurotransmitters or related markers, as well as released neurotransmitters. However, in contrast to neurospheres grown from the brain, the bone marrow-derived NS-MSCs showed a low capacity for differentiating into astrocytes. When rat MSCs-derived neural progenitor-like cells were transplanted into a rat focal ischemia model, they showed a much higher efficiency survival, distribution, and integration in the host brain compared with using naive MSCs. They became postmitotic and adapted well to the host microenvironment to differentiate into cells that were positive for dopaminergic, glutamatergic, and γ-amino butyric acid(GABA)ergic neuronal cell markers. Significant behavioral recovery was recognized in the limb-placing and water-maze tests. In addition, tumor formation was not observed up to 100 days after transplantation as judged by histologic analysis.

As MSCs are useful cells in that they can be obtained easily from patients or a bone marrow bank and can be expanded in culture with fewer ethical problems, our finding offers a new efficient *in vitro* neural progenitor differentiation method to provide a realistic source of neuronal cells for cell therapy.

Materials and methods

Preparation of Marrow Stromal Cells and Neural Induction

The usage of human MSCs for the experiment was approved by the Kyoto University Graduate School and Faculty of Medicine, Ethics Committee. All animal experiments were approved by the Animal Care and Experimentation Committee of the Kyoto University Graduate School of Medicine. Human MSCs were purchased from Cambrex (East Rutherford, NJ, USA). Rat MSCs were harvested according to methods published earlier (Dezawa *et al*, 2001). Both rat and human MSCs were maintained in α-MEM (α-minimum essential medium) (Sigma, St Louis, MO, USA) containing 10% fetal calf serum (FCS) and kanamycin at 37°C with 5% carbon dioxide (CO_2). Rat and human MSCs were then transfected with a vector (pCI neo-NICD) containing the mouse NICD (the NICD cDNA coded for a transmembrane region that included a small fragment of the extracellular domain, followed by a sequence encoding the entire intracellular domain of mouse Notch, initiating at amino acid 1,703 and terminating at the 3′-untranslated sequence). This fragment was subcloned into a pCI-neo vector (Promega Corp., Madison, WI, USA) and was transfected with MSCs using Lipofectamine 2000 (Invitrogen Corp., Carlsbad, CA, USA) and selected by G418 (Invitrogen Corp.) for 7 days, according to the manufacturer's instructions.

Sphere Formation

After G418 selection, both rat and human NICD-transfected cells (referred to as NICD-MSCs) were washed and cultured in α-MEM containing 10% fetal calf serum for 2 days for recovery. After recovery for 2 days, cells were washed and subjected to the free-floating culture for 8 days to generate spheres (referred to as NS-MSCs); i.e., neurobasal medium (Invitrogen Corp.) supplemented with B27 supplement (Invitrogen Corp.), 20 ng/mL bFGF (basic fibroblast growth factor) (R&D Systems Inc., Minneapolis, MN, USA) and 20 ng/mL epidermal growth factor (EGF) (R&D Systems Inc.) at a cell density of 1×10^5 cells per mL on low cell-binding dishes (Nalgene Nunc, Rochester, NY, USA) (Takagi *et al*, 2005). For transplantation, rat spheres, NS-MSCs, were collected and transplanted into the rat (MCAo) middle cerebral artery occlusion model 8 days after the free-floating culture system.

For the differentiation of rat and human NS-MSCs into neuron-like cells *in vitro*, spheres were isolated manually and plated onto laminin (BD Sciences, Bedford, MA, USA) coated slides in a neurobasal medium containing the B27 supplement, 1% fetal bovine serum (FBS) by withdrawal of

EGF and by the addition of 10 μmol/L Forskolin (Calbiochem, La Jolla, CA, USA), 20 ng/mL CNTF (ciliary neurotrophic factor) (R&D Systems Inc.), and 20 ng/mL bFGF (Dezawa *et al*, 2004). After 1 week of culture, cells were fixed and evaluated by immunocytochemistry. To examine the ability to form secondary to fourth spheres, rat and human NS-MSCs were dissociated into single cells and cultured in the free-floating culture system for 8 days in each step.

Induction of Permanent Focal Cerebral Ischemia

Permanent focal cerebral ischemia was induced in 10-week-old male Wister rats using the intraluminal filament technique according to the modified procedure of Koizumi *et al* (1986) and Ohta *et al* (2006). Details of the procedure are available in Supplementary Information.

Transplantation

Three days after MCAo, under inhalational anesthesia with 2% halothane, the rats were fixed in a stereotaxic frame (Narishige, Tokyo, Japan). During the expansion and recovery of rat NICD-MSCs after G418 selection, and green fluorescent protein (GFP) lentivirus was added to the culture medium for 2 days for the labeling of rat NICD-MSCs as described earlier (Nguyen *et al*, 2005; Shimizu *et al*, 2007). After GFP-lentivirus infection, they were subjected to the free-floating culture system to generate rat NS-MSCs, and were injected as spheres into the following places using an electric injector (Muromachi Kikai Co., Tokyo, Japan): 3.5×10^4 cells per 7 μL of rat NS-MSCs into the striatum (from the bregma: anterior (A) 0.0 mm, right (R) +2.0 mm, ventral (V) −4.5 mm, incisor bar −3.3 mm) and 1.5×10^4 cells per 3 μL of those (from the bregma: A 0.0 mm, R +2.0 mm, V −2.0 mm, incisor bar −3.3 mm) into the cortex along the same tract using a Hamilton microsyringe (Hamilton Company, Reno, NV, USA) fitted with a 26-gauge blunt needle. For the control experiment, naive rat MSCs transplantation (cells which were dissociated into a single cell with trypsin were transplanted in the same manner as described above) and vehicle injection (7 and 3 μL of α-MEM into the striatum and cortex, respectively) were performed. The distribution of animals was NS-MSCs ($n = 13$), MSCs ($n = 9$), vehicle ($n = 11$).

Measurement of Lesion Volume

At 100 days after transplantation, animals were perfused through the heart with cold saline and 4% paraformaldehyde in 0.1 mol/L PBS (phosphate-buffered saline) under deep anesthesia (overdose of pentobarbiturate). The brains were cut coronally at 2-mm intervals. Detailed methods of calculating the lesion volume are described in Supplementary Information.

Retrograde Tracer Labeling

Retrograde tracer labeling with Fluorogold (Molecular Probes, Carlsbad, CA, USA) was performed as described earlier (Hayashi *et al*, 2006). Briefly, at 7 days before transcardiac perfusion, the rats received an injection of 0.1 μL of hydroxyl stilbamidine (equivalent to Fluorogold) into the substantia nigra (from the bregma: A −5.0 mm, R +2.3 mm, V −8.25 mm incisor bar −3.3 mm) on the grafted side through a 26-gauge Hamilton microsyringe under general anesthesia.

Antibodies

Primary antibodies used in immunocytochemistry and immunohistochemistry are listed in Table 1. Secondary

Table 1 List of primary antibodies

Primary antibody	*Secondary antibody*	*Company*	*Dilution*
Green fluorescent protein (GFP)	Rabbit IgG	Abcam, Cambridge, MA, USA	1:400
Green fluorescent protein (GFP)	Mouse IgG	Molecular Probes	1:500
β-Tubulin class III (Tuj-1)	Mouse IgG	Sigma	1:800
MAP2ab	Mouse IgG	Sigma	1:1,000
Parvalbumin	Mouse IgG	Sigma	1:2,000
γ-Amino butyric acid (GABA)	Rabbit IgG	Sigma	1:200
Glial fibrillary acidic protein (GFAP)	Rabbit IgG	DAKO, Caspenteria, CA, USA	1:300
Glial fibrillary acidic protein (GFAP)	Mouse IgG	Chemicon	1:200
Sox2	Rabbit IgG	Chemicon	1:200
NeuroD	Rabbit IgG	Chemicon	1:200
NeuN	Mouse IgG	Chemicon	1:200
Tyrosine hydroxylase (TH)	Rabbit IgG	Chemicon	1:1,000
Dopamine transporter (DAT)	Rabbit IgG	Chemicon	1:200
Glutamate	Rabbit IgG	Chemicon	1:200
Calbindin	Rabbit IgG	Chemicon	1:500
DARPP32	Rabbit IgG	Chemicon	1:500
Choline acetyl transferase (ChAT)	Rabbit IgG	Chemicon	1:1,000
Serotonin (5-HT)	Rabbit IgG	ImmunoStar	1:2,000
Glutamic acid decarboxylase (GAD)	Rabbit IgG	Chemicon	1:1,000
Synaptophysin	Mouse IgG	Chemicon	1:1,000
Nestin	Mouse IgG	BD Pharmingen, San Jose, CA, USA	1:400
Ki-67	Rabbit IgG	Thermo, Waltham, MA, USA	1:200

IgG, immunoglobulin G; MAP2ab, microtubule associated protein 2.

antibodies used were antirabbit IgG (immunoglobulin G) conjugated either to Alexa Fluor 488 or 568, and antimouse IgG conjugated either to Alexa Fluor 488 or 568 (1:500; Molecular Probes, Carlsbad, CA, USA).

Immunocytochemistry

Differentiated cells from rat and human NS-MSCs were fixed with 4% paraformaldehyde in 0.1 mol/L PBS. Spheres derived from rat and human MSCs were fixed with 4% paraformaldehyde, cryoprotected in a series of sucrose solutions (15, 20, and 25% sucrose in 0.02 mol/L PBS) at 4°C for 2 days, and then cut into 10-μm-thick sections using cryostat (Leica CM 1850, Wetzlar, Germany). A detailed procedure of immunocytochemistry is described in Supplementary Information.

The total number of cells was evaluated by counting of 4′, 6-diamidino-2-phenylindole- (DAPI)-positive nuclei, and the percentage of immunoreactive cells was evaluated using the Nikon confocal microscope system C1si (Nikon Corporation, Tokyo, Japan). The cells in five fields, which include 100 to 500 cells, were counted for three independent cultures.

Western Blot

pCI-neo-NICD-GFP vector was constructed by the insertion of EGFP gene fragment (Promega Corp.) into the pCI-neo-NICD vector. Six, 12, 24, 36, 48 h and 3 and 5 days after the introduction of pCI-neo-NICD-GFP plasmid by Lipofectamine 2000, cells were harvested and subjected to western blot analysis as described in Supplementary Information. G418 was administrated from 48 h to 5 days after lipofection for the selection of the transfected cells.

Reverse Transcription-PCR

To analyze the relative expression of different mRNAs, the amount of cDNA was normalized on the basis of the signal from ubiquitously expressed β-actin. Primer sequences and precise conditions are β-actin: 5′-AACTGGGACGATATG GAGAA-3′ (forward) and 5′-GTAACCCTCATAGATGGG CA-3′(reverse) (TM, melting temperature; 66°C, 25 cycles); neuron-specific enolase (NSE): 5′-GGTGAAGGAAGCCA TTGACAA-3′ (forward) and 5′-ATGCCGACATTGGCTGT GA-3′ (reverse) (TM, melting temperature; 66°C, 27 cycles); and choline acetyltransferase (ChAT): 5′-GGAGCTAT TCCTCTTTCGGGATT-3′ (forward) and 5′-GTCAGTCATG GCTTGCACAAA-3′ (reverse) (TM; 66°C, 40 cycles). Total RNA of rat adult brain was used in the reaction of the positive control for each factor.

HPLC (High Performance Liquid Chromatograph)

NS-MSCs cultured in the free-floating culture system for 7 days were replated and cultured in α-MEM with 1% serum, 10 μmol/L Forskolin, 20 ng/mL CNTF, and 20 ng/mL bFGF, followed by the administration of glial cell line-derived neurotrophic factor (50 ng/mL) for 5 days. The concentration of dopamine release was determined by HPLC using a reverse-phase column and an electrochemical detector system (Eicom, Kyoto, Japan) as described earlier (Dezawa *et al*, 2004). Details of the procedure are available in Supplementary Information.

Behavioral Analysis

The limb-placing test was a modified version of a test described by De Ryck *et al* (1989) and Jeong *et al* (2003). The test was performed the day before ischemia induction and after transplantation on days 4, 10, 14, 21, 28, 56 and 84. The total score ranged from 0 to 7.

The Morris water-maze test was performed as described earlier (Mimura *et al*, 2005; Morris, 1984). This test was performed from day 96 to day 100 after transplantation. Each detailed procedure is described in Supplementary Information. After behavioral follow-up, at 100 days after transplantation, each animal underwent perfusion fixation under anesthesia. In all, 10-μm-thick brain cryosections were prepared by cryostat. As for the positive control, normal rats ($n = 8$) were used.

Immunohistochemistry

In 14 and 100 days after transplantation, each animal was perfused through the heart with cold saline and 4% paraformaldehyde in 0.1 mol/L PBS under deep anesthesia (overdose of pentobarbiturate). The brains were cut coronally at 2-mm intervals, and 6 brain slices were prepared totally. Each brain slice was cut into 10-μm-thick coronal sections using a cryostat, and one cryosection was chosen from each slice. Transplanted cells of 10 fields in each cryosection were counted using the Nikon confocal microscope system C1si for three animals, and the cell number of positive cells in serial sections was calculated. Cells of thickness larger than 10-μm could have been counted multiple times. For this, the size and thickness of cells were corrected using the Abercrombie method for controlling the bias in counting (Abercrombie, 1946).

Details of the immunostaining procedure are described in Supplementary Information. The samples were inspected under Nikon confocal microscope system C1si.

The numbers of animals subjected to experiments were NS-MSCs = 13, MSCs = 9, vehicle = 11 (for 100 days after transplantation), and NS-MSCs = 8, MSCs = 8 (for 14 days after transplantation).

Real-Time PCR

Total RNA was collected using the RNeasy Mini Kit (Qiagen GmbH, Hilden, Germany), and cDNA was synthesized using High Capacity cDNA Reverse Transcription Kit (Applied Biosystems, Foster City, CA, USA). Primers and probes for NSE (γ, γ-enolase), sodium channel voltage-gated type III Scn3a, and β-actin were purchased from TaqMan Gene Expression Assay (Applied Biosystems) and subjected to real-time PCR according to the manufacturer's instructions.

To estimate the number of transplanted cells that survived and integrated in the host tissue 100 days after

grafting, real-time PCR was performed using a 7300 sequence detection system (Applied Biosystems). Real-time PCR primers and the probe for GFP used in this study were 5′-AGTCCGCCCTGAGCAAAGA-3′ and 5′-TCCAGC AGGACCATGTGATC-3′, and 5′-FAM-CCCAACGAGAAG CG-MGB-3′, respectively. Standard curves were generated by serially diluting cDNA derived from cultured MSCs. Values were normalized by assays for β-actin using TaqMan β-actin Detection Reagents (Applied Biosystems).

Statistical Analysis

Data are expressed as mean ± s.e.m. Data were compared using ANOVA (analysis of variance) with pairwise comparisons by the Bonferroni method. As the score of the limb-placing test is ordinal (i.e., 8 levels (0 to 7)), the Mann–Whitney *U*-test was chosen for the nonparametric statistical analysis of the limb-placing test.

Results

Generation of Spheres from Marrow Stromal Cells

After NICD transfection into MSCs (NICD-MSCs), morphologic changes were observed, i.e., the cells became smaller (Figures 1A and 1B). These NICD-MSCs were subjected to the free-floating culture system (neurobasal medium supplemented with B27, bFGF, and EGF for 8 days) to form spheres (NS-MSCs, Figure 1C). Naive MSCs formed spheres but the efficiency was very low compared with that of both rat and human NICD-MSCs; in rats, NICD-MSCs produced seven times more spheres (~35 spheres per 10,000 cells) than did naive MSCs (~5 spheres per 10,000 cells), and in humans, NICD-MSCs produced ~50 spheres per 10,000 cells in all clones examined, whereas naive MSCs produced 0 to 4 spheres per 10,000 cells. The diameter of the NS-MSCs spheres was ~60 to 150 μm, whereas that of MSCs was mostly under 60 μm. Rat and human NS-MSCs were dissociated and subjected to secondary, third, and fourth sphere formation. Eight days after replating, secondary spheres could be recognized but few third and no fourth generation were observed (data not shown). In this regard, the sphere formation of NS-MSCs is limited.

To determine whether the spheres contained cells with neural progenitor properties, we examined the expression of Sox2, nestin, and NeuroD. In naive rat MSCs, a few cells were positive for Sox2 (2.0 ± 1.4%), nestin (2.3 ± 0.9%), and NeuroD (9.4 ± 2.2%). In contrast, induced spheres contained much higher percentages of cells positive for nestin (61 ± 4.8%), NeuroD (96.8 ± 0.9%), and Sox2 (93.9 ± 2.4%) (Figures 1D–1F). Almost identical data were obtained from human MSCs.

To examine whether cells in the spheres were committed to a neural lineage cell, spheres were dissociated, replated to adherent dishes, and then differentiated *in vitro* by low serum and withdrawal

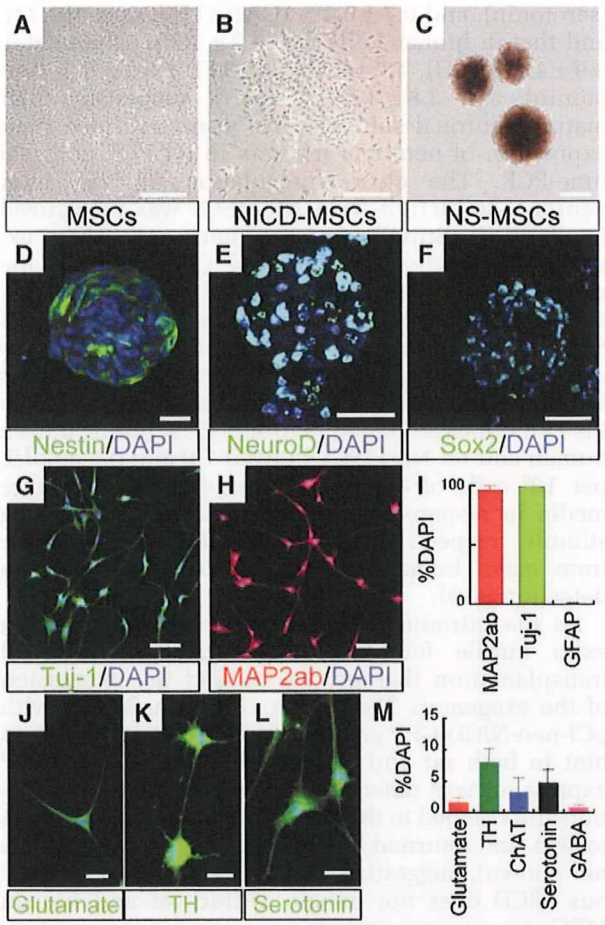

Figure 1 Neuronal induction from marrow stromal cells (MSCs). (**A–C**) Phase-contrast images of rat cells. After Notch intracellular domain (NICD) transfection, original naive MSCs (panel A) changed their morphology (NICD-MSCs, panel B). Panel C represents spheres made from NICD-MSCs (refereed to as NS-MSCs) on a low cell-binding dish. (**D–F**) Expression of nestin (panel D), NeuroD (panel E), and Sox2 (panel F) in rat NS-MSCs. (**G** and **H**) β-tubulin isotype III (Tuj-1)- (panel G) and microtubule associated protein 2 (MAP2ab)-positive (panel H) neuron-like cells differentiated from rat NS-MSCs. (**I**) The proportions of rat cells expressing neural markers. (**J–L**) Expression of glutamate (panel J), tyrosine hydroxylase (TH) (panel K), and serotonin (panel L) in neuron-like cells derived from rat NS-MSCs spheres. The proportions of cells expressing neurotransmitter-related markers in rat cells (**M**). Scale bars = 250 μm (panels A and B), 100 μm (panel C), 50 μm (panels D–F), 20 μm (panels J–L).

of EGF. Adhered rat and human cells had neurite-like processes with abundant varicosities and were immunoreactive to markers of neuronal cells, β-tubulin isotype III (Tuj-1) (98.5 ± 0.5%) and microtubule associated protein 2 (MAP-2) (95.7 ± 3.7%) (Figures 1G–1I). A very small number of cells were immunopositive for the astrocyte marker, glial fibrillary acidic protein (0.7 ± 0.3%). The expression of transmitter-related markers in rat cells was 1.6 ± 0.7% (glutamate), 7.9 ± 2.2% (TH (tyrosine hydroxylase)), 3.2 ± 2.3% (ChAT), 4.7 ± 2.3%

(serotonin), and 0.7 ± 0.4% (GABA) (Figures 1J–1M), and that in human cells was 8.2 ± 5.7% (glutamate), 8.9 ± 4.1% (TH), 4.7 ± 2.4% (ChAT), 3.8 ± 2.9% (serotonin), and 3.8 ± 3.7% (GABA), suggesting their mature neuronal subtypes. We also confirmed their expression of neuronal markers in RT-PCR and real time-PCR. The clear upregulation of NSE after neuronal induction from NS-MSCs was recognized in RT-PCR (Supplementary Figure 1). They expressed not only NSE but also ChAT, one of the markers for functional neurons. In real-time PCR, both NSE and voltage-gated sodium channel type III Scn3a were shown to be substantially upregulated or expressed in neuronal cells induced from NS-MSCs but not in naive MSCs (Supplementary Figure 2). In the HPLC measurement, neuronal cells induced from human and rat NS-MSCs showed 1.0 and 0.5 pmol/L per 10^6 cells of dopamine release into the culture media in response to high potassium depolarizing stimuli, respectively, whereas dopamine release from naive human and rat MSCs was under the detection level.

As the introduction of an exogenous gene is an extra hurdle for the safety aspect in the cell transplantation therapy, we tracked the expression of the exogenous *NICD* gene after transfection with pCI-neo-NICD-GFP genes at protein level by western blot in both rat and human MSCs. The NICD-GFP expression was detectable from 12 h after introduction and reached to the maximum expression from 24 to 48 h, and returned to the basal level by 5 days (data not shown), suggesting that the introduced exogenous NICD does not remain within rat and human MSCs for a longer period.

Transplantation of NS-MSCs into Focal Cerebral Ischemic Lesions

To evaluate whether NS-MSCs were able to integrate into the host brain and contribute to the amelioration of the neurodegeneration, we transplanted the rat NS-MSCs into a rat model of permanent focal cerebral ischemia. All rats exposed to focal cerebral ischemia had areas of severe corticostriatal infarction. Each animal received 50,000 cells, which were transplanted into the striatum and cortex after 3 days of MCAo. For control groups, the same number of naive MSCs (MSCs) or vehicle was injected.

The tissue defect observed in each experimental group was defined as the lesion. The mean lesion volumes in the NS-MSCs, MSCs, and vehicle groups on day 100 were 27.1 ± 4.3%, 23.0 ± 2.3%, and 31.4 ± 5.0%, respectively. There was no statistical difference among groups.

Limb-Placing Test

Rats with focal cerebral ischemia initially showed severe impairment in the limb-placing test (Figure 2A). From days 4 to 84 after transplantation,

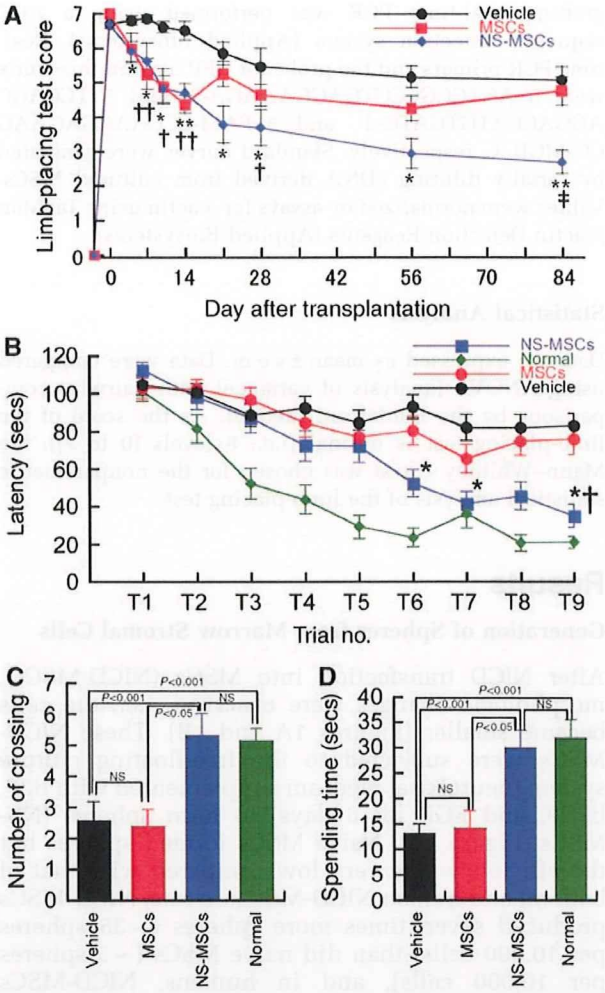

Figure 2 Behavioral analysis. (**A**) Limb placing. Mean scores for the NS-MSCs group were statistically different from those of the marrow stromal cells (MSCs) group at day 84. Mean scores for the MSCs group were also significantly different from those of the vehicle group from days 10 to 14 and at day 28, but not at day 21 and from days 56 to 84. (*NS-MSCs versus vehicle, †MSCs versus vehicle, ‡NS-MSCs versus MSCs, $P < 0.05$, **,††, $P < 0.001$) (**B**) Morris water-maze test. The mean latency of the NS-MSCs group to locate the platform was significantly different from that of the MSCs (*) or vehicle (†) groups. (*,†$P < 0.05$, **$P < 0.001$) (**C**) The result of water-maze spatial probe trial. The duration of time the rat swam through the area, in which the platform was located earlier. (**D**) The time spent in the quadrant, in which the platform was located earlier in the water maze. These values for the NS-MSCs group are significantly different from those of the MSCs or vehicle groups. NS, nonsignificant.

the mean score of the NS-MSCs group was significantly improved compared with that of the vehicle group, indicating that the NS-MSCs group significantly induced long-term behavioral recovery. The mean score of the NS-MSCs group was also significantly improved compared with that of the MSCs group at day 84. In contrast, the MSCs group showed

significantly improved performance compared with the vehicle group only on days 10 to 14 and 28. At days 21 and 56 to 84, there was no significant difference between the MSCs and vehicle groups.

Water-Maze Test

The mean latency time recorded for NS-MSCs, MSCs, vehicle, and normal groups is presented in Figure 2B. The NS-MSCs group had a significantly shorter latency time to reach the escape platform than the MSCs and vehicle groups. In the spatial probe test, the number of platform location crossings and the amount of time spent in the target quadrant were significantly longer in the NS-MSCs group compared with that in the MSCs and vehicle groups (Figures 2C and 2D) again suggesting a functional effect of the NS-MSC grafted cells. There was no statistical difference between NS-MSCs and normal rats.

Histologic Analysis

Cells were labeled with GFP lentivirus before transplantation. Tumor formation, a massive occupying effect in the brain tissue as in the case of embryonic stem cell transplantation (Takagi *et al*, 2005), could not be observed in the grafted brain during the 100-day follow-up in all groups, including NS-MSC grafted rats. Green fluorescent protein-positive NS-MSCs were widely observed at the lesion boundary, ipsilateral cortex, and striatum but most intensively around the lesion site (Figure 3A). Their migration was confined to the ipsilateral site, and GFP-positive NS-MSCs were not detected in the contralateral side. In the NS-MSCs group at day 100, $21 \pm 1.3 \times 10^4$ GFP-labeled cells survived. On the basis of the initial number of transplanted cells (5×10^4), the NS-MSCs appeared to have proliferated after transplantation. Among the GFP-labeled cells, $4.7 \pm 0.02\%$ were immunoreactive for Ki67 at day 14, but Ki67-positive cells were not observed at 100 days, suggesting that the cells did not continue to divide. In the MSCs group, in contrast, there were $1.3 \pm 0.46 \times 10^4$ GFP-positive cells at day 100 and these were mostly detected around the injected area, and rarely observed to be migrating through the parenchyma in the cortex or the striatum (Figure 3A). Furthermore, a successful neuronal differentiation was not observed in the MSCs group. To further confirm the difference in GFP-positive cell numbers between the NS-MSCs and MSCs groups, we performed real-time PCR for the GFP gene. At day 100, the NS-MSCs-transplanted brain showed a 19.6 ± 6.9 times greater GFP gene content compared with the MSCs-transplanted brain.

To determine whether transplanted cells expressed neural markers, sections were immunostained with NeuN and glial fibrillary acidic protein antibodies. In the NS-MSCs group, the percentages of GFP-positive cells that were NeuN- and glial fibrillary acidic protein-positive were $79.5 \pm 0.1\%$ (Figures 3B–3D) and $1.9 \pm 0.03\%$ (data not shown), respectively. In the MSCs group, neither NeuN- nor glial fibrillary acidic protein-positive cells were detected (data not shown). The number of GFP-positive cells in the NS-MSCs and MSCs groups in each section was counted from the anterior to the posterior of the brain. Remarkably, NS-MSCs were observed widely in the antero-posterior axis throughout the brain, in addition to the transplanted site, whereas only a small number of transplanted MSCs were identified, and these were located only around the lesion.

The expression of differentiation markers and neurotransmitter-related markers in NS-MSCs was then examined. The GFP-positive cells were also immunoreactive to dopamine transporter ($32.8 \pm 11.4\%$), TH ($41.4 \pm 17.6\%$), glutamic acid decarboxylase ($10.2 \pm 5.7\%$), glutamate ($4.1 \pm 0.4\%$), calbindin ($7.7 \pm 2.5\%$), DARPP32 ($13.1 \pm 12.5\%$), and parvalbumin ($18.9 \pm 9.9\%$) (Figure 4).

Fluorogold Tracing and Synaptophysin Staining

To assess the possibility that the transplanted NS-MSCs extended neurites with active transport capacity in the host brain, we injected a retrograde tracer at 93 days after transplantation. Fluorogold was injected into the substantia nigra, and then the grafted area was subjected to Fluorogold detection at 100 days. Of the GFP-positive cells, $35.2 \pm 7.3\%$ of the cells were Fluorogold-positive and had a neuron-like morphology (Figures 5A–5F). We also investigated the expression of synaptophysin, and $15.78 \pm 2.94\%$ of GFP-positive cells showed synaptophysin positivity in the striatum (Figures 5G–5J). These data suggest that grafted cells extended long processes from the striatum to the substantia nigra and some of these expressed the synaptic marker synaptophysin.

Discussion

In this study, we report that committed neural progenitor cells, NS-MSCs, can be efficiently differentiated from rat and human MSCs by NICD introduction followed by the free-floating culture system that promotes the formation of spheres. Cells in these spheres expressed markers related to neural progenitor cells, and were shown to be committed to neural lineage cells by immunocytochemistry and grafting into the brain. NS-MSCs also differentiated into neuronal cells after transplantation into a rat focal cerebral ischemia model, and were shown to be immunoreactive to various neurotransmitter-related markers within the host tissue, suggesting their potential to differentiate into various types of neuronal cells. Their contribution to functional recovery was also observed for up to 100 days after transplantation. Importantly, no tumors were detected. On the basis of these results, NS-MSCs may

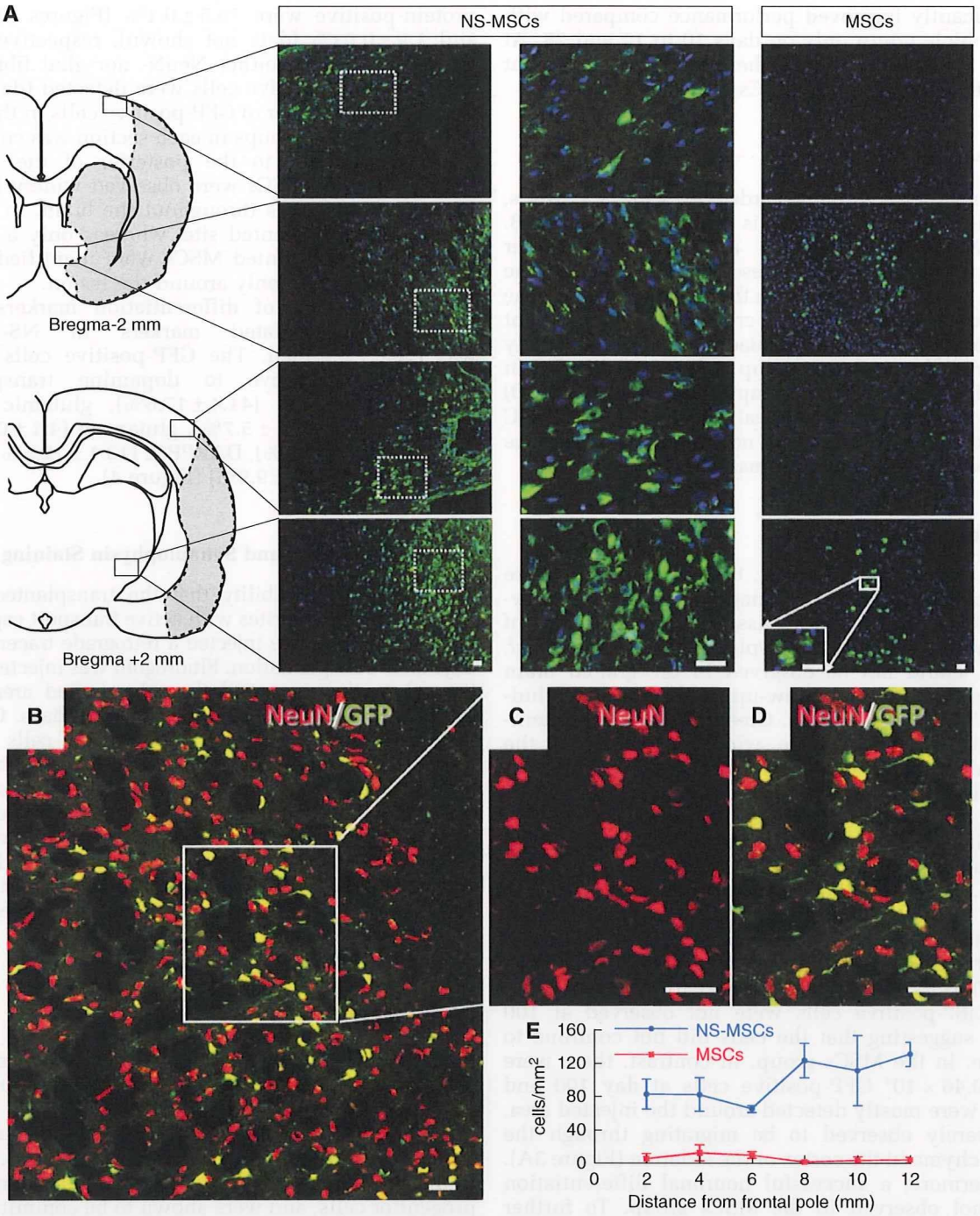

Figure 3 Transplanted cells in the brain lesion (day 100). (**A**) Distribution of transplanted NS-MSCs and marrow stromal cells (MSCs). In the ischemic boundary zone, a number of green fluorescent protein (GFP)-positive cells were observed in the NS-MSCs group. In the MSCs group, a small number of GFP-positive cells were observed, mostly small cells without extended processes. (**B–D**) NeuN-positive cells in NS-MSCs. (**E**) The number of GFP-positive cells in NS-MSCs and MSCs groups in each section from the anterior pole to the dorsal side of the brains. Scale bars = 20 μm.

be a good source of neuronal lineage cells for cell transplantation therapy in stroke.

Accumulating evidence shows that naive MSCs transplantation into the ischemic brain leads to improved behavior (Chen and Chopp, 2006; Li *et al*, 2002). According to these reports, the survival rate of MSCs in the host brain was under 10%, and the proportion showing neuronal differentiation was

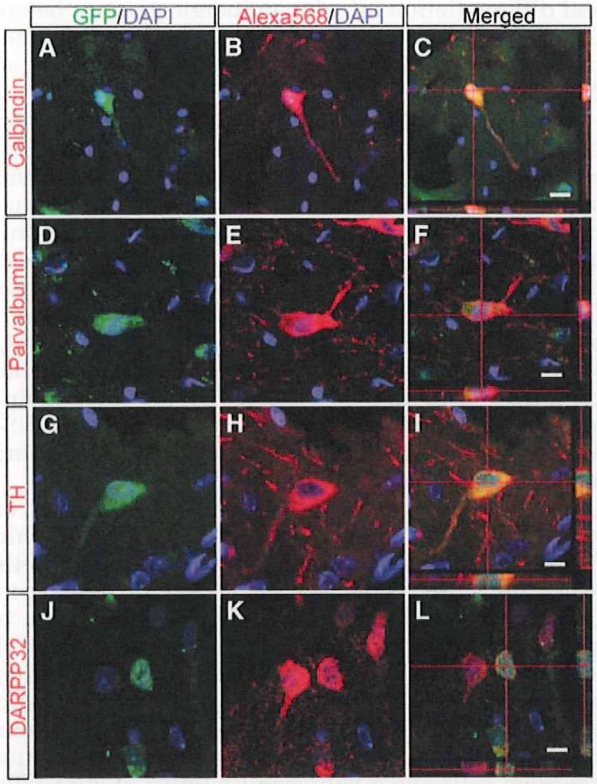

Figure 4 Immunohistochemistry of green fluorescent protein (GFP)-positive transplanted NS-MSCs (day 100). (**A**–**C**) Calbindin, (**D**–**F**) parvalbumin, (**G**–**I**) tyrosine hydroxylase (TH), (**J**–**L**) DARPP32. These cells are mostly observed in the lesion boundary. Scale bars = 20 μm.

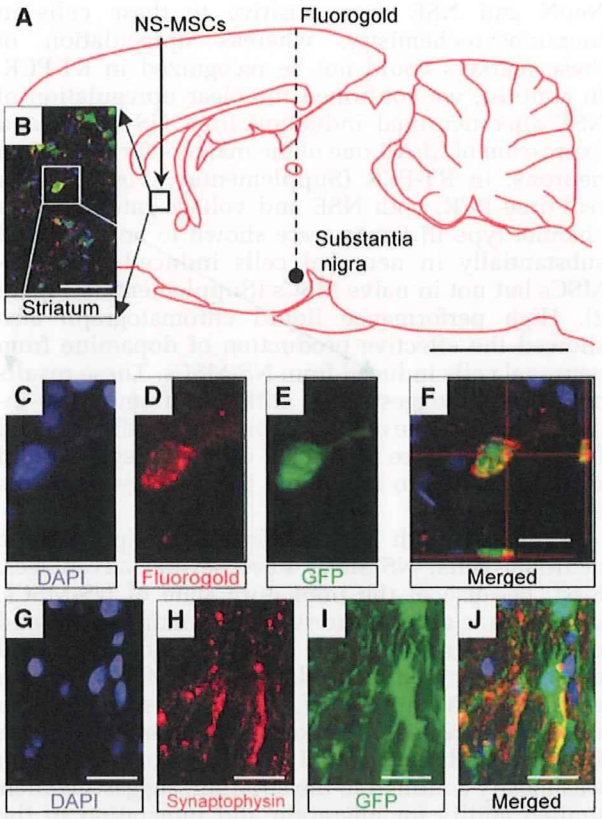

Figure 5 The expression of retrograde tracer Fluorogold injected in the targeted area of the substantia nigra and synaptophysin expression in the graft (day 100). (**A**) Site of NS-MSCs transplantation and Fluorogold injection. (**B**) Immunohistochemistry showed Fluorogold and green fluorescent protein (GFP) double-positive cells in the striatum. Higher magnification of 4′,6-diamidino-2-phenylindole (DAPI) (**C**), Fluorogold (**D**), and GFP (**E**) double-positive cells (**F**) with neuron-like morphology. (**G**–**J**) Synaptophysin is expressed in the perisynaptic areas of GFP-positive transplanted cells in the striatum. Scale bars = 5 mm (panel A), 100 μm (panel B), and 20 μm (panels C–J).

1% to 2%. The functional recovery induced by these naive MSCs transplantation may partly be mediated by the trophic effects of MSCs or by the intrinsic parenchymal cells stimulated by MSCs (Chen and Chopp, 2006; Li *et al*, 2002). However, in this study, a large number of GFP-labeled NS-MSCs was measured in the host brain even after 100 days of transplantation, and most of the cells expressed neuronal markers and neurotransmitter-related markers. In addition, Fluorogold tracing showed that the transplanted cells extended neurites for some distance in the host brain and might have formed synapses with host neurons. The true contribution of the neurite extension of transplanted NS-MSCs remains unclear; although our results suggest that the differentiation or orientation of MSCs into cells with neural properties before transplantation is effective for the survival and integration of MSCs.

In our result, recovery occurs long before the cells can have integrated into the host brain. In the limb-placing test, the MSC group showed slight recovery in the earlier period after operation, and the mean lesion volumes between the NS-MSCs and MSCs groups showed no statistical difference. Perhaps, the recovery in the earlier period (before 14 days) resulted from the trophic effect of transplanted cells rather than from the replenishment of lost cells. As mentioned above, naive MSCs are known to have trophic effects and therefore, it is no wonder that NS-MSCs also procure the same effect. However, in the later period, MSCs do not survive, whereas NS-MSCs do, which are migrated and differentiated in the host tissue. Although the cell replacement by transplanted NS-MSCs cannot be the entire contribution for the functional recovery, this difference may explain the functional recovery shown in NS-MSCs groups at a later period of 100 days.

Under stressful conditions, MSCs are shown to exhibit neuron-like morphology and to express neuronal markers, but without ever having undergone protein synthesis, indicating that the neuron-like morphologic and immunocytochemical changes are artifacts (Lu *et al*, 2004). Indeed, in their report,

NeuN and NSE were positive to these cells in immunocytochemistry, whereas upregulation of these markers could not be recognized in RT-PCR. In contrast, we confirmed the clear upregulation of NSE after neuronal induction from NS-MSCs, and expression of ChAT, one of the markers for functional neurons, in RT-PCR (Supplementary Figure 1). In real-time PCR, both NSE and voltage-gated sodium channel type III Scn3a were shown to be expressed substantially in neuronal cells induced from NS-MSCs but not in naive MSCs (Supplementary Figure 2). High performance liquid chromatograph also showed the effective production of dopamine from neuronal cells induced from NS-MSCs. These results collectively suggest that, different from stress-induced neuron-like cells, neuronal cells differentiated from NS-MSCs are functional as the upregulation of markers related to functional neurons are shown as described above.

Compared with fully differentiated postmitotic neuronal cells, NS-MSCs have several advantages. First, because of the premature state of NS-MSCs, they have a greater survival rate, distribution, and integration in the host brain. For differentiated dopaminergic neurons induced from MSCs (Dezawa *et al*, 2004; Mimura *et al*, 2005), the survival ratio was only 20% to 30% after transplantation into the Parkinson's disease model rat and their distribution was mostly confined to the striatum, suggesting their limited ability for migration and integration in the host tissue. However, NS-MSCs were widely observed in the lesion boundary, ipsilateral cortex, and striatum in the stroke brain and $21 \pm 1.3 \times 10^4$ cells were counted after the transplantation of 50,000 cells. As 4.7% of GFP-positive NS-MSCs were positive for Ki67 at 14 days, but GFP-positive cells were negative for Ki67 at 100 days, a subpopulation of NS-MSCs might have proliferated at an earlier period, but most of them became postmitotic by day 100. These observations might partly explain the following: (1) the ability of NS-MSCs to proliferate and migrate because of their premature state and (2) although NS-MSCs show neural lineage commitment *in vitro*, their differentiation into functional neuronal subtypes in the host tissue, such as dopaminergic, glutamatergic, and GABAergic marker-positive cells might subsequently be regulated by the host microenvironment.

Second, NS-MSCs differentiated into various kinds of transmitter-related marker positive cells within the host brain. They also extended neurites for a long distance for ~6.3 mm. This suggests that premature NS-MSCs have higher flexibility to adapt to the host microenvironment and to differentiate into various cell types rather than fully differentiated neuronal cells. Such properties would be beneficial when replenishing neural cells are required to cover a large degenerated region and various types of neural cells are required, such as in the case of stroke. Conversely, in Parkinson's disease, as dopamine-producing cells are the main target, induction and differentiation into dopaminergic neurons before the transplantation would be preferable for functional recovery (Dezawa *et al*, 2004; Mimura *et al*, 2005).

Third, NS-MSCs are more easily prepared than fully differentiated neuronal cells, which might be beneficial from a practical aspect. Precise control and maintenance are required to achieve the differentiation of neuronal cells from human MSCs, appropriate density in the case of seeding and pertinent harvesting method. As for the NS-MSCs method, this free-floating culture method is not highly dependent on cell density and does not require harvesting. Moreover, in general, mature neurons are vulnerable compared with neural progenitors for their maintenance. Considering these three aspects, the NS-MSCs method will clinically be feasible for treating acute injuries like stroke.

Earlier reports have described the induction of neurosphere-like cells from MSCs using trophic factors and/or the medium used for neural stem cells (Hermann *et al*, 2004; Lee *et al*, 2003). Notably, in these reports, the ratio of glial cell differentiation is higher than that of neuronal cells; induction rates of mature neurons versus astrocytes derived from neurosphere-like cells are $6 \pm 2\%$:$13 \pm 4\%$ (Hermann *et al*, 2004) or 6.5%:32.9% (Lee *et al*, 2003). In our system, almost all of the NS-MSCs differentiated into neuronal cells and a very small number of glial cells were produced, both *in vitro* and *in vivo*. This finding suggests that NICD introduction and sphere formation strongly shifted the MSCs to a neuronal potential.

The number of GFP-labeled transplanted cells at 100 days after transplantation was four times higher than that at 14 days. Therefore, we conducted the study on Ki67 staining, a marker for cell proliferation related to tumor genesis, which showed that Ki67-positive cells were detected in 14 but not in 100 days. Furthermore, the percentage of GFP-positive cells that expressed NeuN at 100 days was very high ($79.5 \pm 0.1\%$). Some of them might get disposed from the organism after transplantation, but overall, this result suggests that large number of Ki67-positive cells at 14 days did not continue to divide and differentiated into neuronal phenotype by 100 days. Consistently, the ability to generate spheres was limited in NS-MSCs, i.e., NS-MSCs could generate second and third spheres but were unable to show fourth sphere formation. In addition, tumor formation was not detected up to 100 days. Many reports suggested that MSCs are less tumorigenic than fetus-derived stem cells or embryonic stem cells, and few reports with regard to MSC transplantation into stroke model animals reported ectopic tissue formation or carcinogenesis (Chen *et al*, 2001*a*, *b*). Indeed, these earlier reports do not completely cast aside the tumorigenic possibility of MSC or MSC-derived cells. The most reliable safety evaluation will not be performed in the rat experiment but in the higher mammals like monkeys; therefore, we recognize that

evaluation in the monkey experiment is necessary in the future.

Notch signaling inhibits neuronal differentiation and promotes glial differentiation during development (Lundkvist and Lendahl, 2001). Although our results seem inconsistent with the well-known action of Notch signaling, it is presumed that cell susceptibility to Notch signaling in MSCs is different from cells in the process of neuronal development. Our results suggest distinct cellular responses to Notch signals; e.g., the protein repertoire and active factors may be quite different between conventional neural progenitor cells and MSCs. We recognized in this experiment that NICD transfection leads to an upregulation of NeuroD in the luciferase assay as described earlier (Dezawa *et al*, 2004), which suggests that, at least in MSCs, cells are orientated to a neural differentiation by NICD introduction. Furthermore, treatment with the free-floating culture system might have selected cells with a high potential for neural differentiation. The precise mechanism underlying the MSCs acquisition of neural progenitor cell properties in this system needs to be clarified.

Several reports indicated that remote degeneration of neurons together with the change in *Bcl-2* and tumor necrosis factor-α expression level occurs in the substantia nigra after focal ischemia (Arango-Davila *et al*, 2004; Loos *et al*, 2003). These observations suggested that the nigrostriatal pathway was damaged after focal ischemia. Earlier reports showed the improvement of behavioral dysfunction after striatal transplantation of embryonic stem cells, which was assessed by methamphetamine injection, the test known to estimate the nigrostriatal pathway (Yanagisawa *et al*, 2006). The result indicated that striatal transplantation could repair the damage of the nigrostriatal pathway. Our result also showed the same effect of striatal transplantation.

Furthermore, several earlier studies indicated that hemispheric damage influenced the result of water-maze test (Puurunen *et al*, 2001; Veizovic *et al*, 2001). In addition, Yonemori *et al* (Yonemori *et al*, 1999) reported that focal cerebral ischemia caused spatial memory disturbance in rats. Therefore, in our experiment, the improvement of this test might have been brought about by the improvement of both cognitive and motor functions.

Human MSCs have a high proliferation ability; 20 to 100 mL of bone marrow aspirate provides 1×10^7 MSCs within several weeks. Considering the sphere formation efficiency described above, as many as 5×10^4 spheres may be obtained from a patient's bone marrow within a reasonable time period. We also confirmed that cryopreserved NS-MSCs could proliferate and repeatedly form spheres while maintaining their neural progenitor-like characteristics (data not shown). Therefore, not only for autologous transplantation, but also for a cell-providing system using the same human leukocyte antigen subtype, MSCs from a healthy donor might be a realistic approach for cell therapy. This MSC cell therapy approach may be applicable for stroke victims and for those of other neurodegenerative diseases.

Acknowledgements

We thank Dr M Bohn (Northwestern University, Chicago) for giving us helpful advice and for editing our paper.

Conflict of interest

The authors declare no conflict of interest.

References

Abercrombie M (1946) Estimation of nuclear population from microtome sections. *Anat Rec* 94:239–47

Arango-Davila CA, Cardona-Gomez GP, Gallego-Gomez JC, Garcia-Segura LM, Pimienta HJ (2004) Down-regulation of Bcl-2 in rat substantia nigra after focal cerebral ischemia. *Neuroreport* 15:1437–41

Bliss T, Guzman R, Daadi M, Steinberg GK (2007) Cell transplantation therapy for stroke. *Stroke* 38:817–26

Borlongan CV, Hadman M, Sanberg CD, Sanberg PR (2004) Central nervous system entry of peripherally injected umbilical cord blood cells is not required for neuroprotection in stroke. *Stroke* 35:2385–9

Chen J, Chopp M (2006) Neurorestorative treatment of stroke: cell and pharmacological approaches. *NeuroRx* 3:466–73

Chen J, Li Y, Wang L, Lu M, Zhang X, Chopp M (2001*a*) Therapeutic benefit of intracerebral transplantation of bone marrow stromal cells after cerebral ischemia in rats. *J Neurol Sci* 189:49–57

Chen J, Sanberg PR, Li Y, Wang L, Lu M, Willing AE, Sanchez-Ramos J, Chopp M (2001*b*) Intravenous administration of human umbilical cord blood reduces behavioral deficits after stroke in rats. *Stroke* 32:2682–8

De Ryck M, Van Reempts J, Borgers M, Wauquier A, Janssen PA (1989) Photochemical stroke model: flunarizine prevents sensorimotor deficits after neocortical infarcts in rats. *Stroke* 20:1383–90

Dezawa M, Hoshino M, Nabeshima Y, Ide C (2005) Marrow stromal cells: implications in health and disease in the nervous system. *Curr Mol Med* 5:723–32

Dezawa M, Kanno H, Hoshino M, Cho H, Matsumoto N, Itokazu Y, Tajima N, Yamada H, Sawada H, Ishikawa H, Mimura T, Kitada M, Suzuki Y, Ide C (2004) Specific induction of neuronal cells from bone marrow stromal cells and application for autologous transplantation. *J Clin Invest* 113:1701–10

Dezawa M, Takahashi I, Esaki M, Takano M, Sawada H (2001) Sciatic nerve regeneration in rats induced by transplantation of in vitro differentiated bone-marrow stromal cells. *Eur J Neurosci* 14:1771–6

Hayashi J, Takagi Y, Fukuda H, Imazato T, Nishimura M, Fujimoto M, Takahashi J, Hashimoto N, Nozaki K (2006) Primate embryonic stem cell-derived neuronal progenitors transplanted into ischemic brain. *J Cereb Blood Flow Metab* 26:906–14

Hermann A, Gastl R, Liebau S, Popa MO, Fiedler J, Boehm BO, Maisel M, Lerche H, Schwarz J, Brenner R, Storch A (2004) Efficient generation of neural stem cell-like cells from adult human bone marrow stromal cells. *J Cell Sci* 117:4411–22

Igura K, Zhang X, Takahashi K, Mitsuru A, Yamaguchi S, Takashi TA (2004) Isolation and characterization of mesenchymal progenitor cells from chorionic villi of human placenta. *Cytotherapy* 6:543–53

In 't Anker PS, Scherjon SA, Kleijburg-van der Keur C, Noort WA, Claas FH, Willemze R, Fibbe WE, Kanhai HH (2003) Amniotic fluid as a novel source of mesenchymal stem cells for therapeutic transplantation. *Blood* 102:1548–9

Jeong SW, Chu K, Jung KH, Kim SU, Kim M, Roh JK (2003) Human neural stem cell transplantation promotes functional recovery in rats with experimental intracerebral hemorrhage. *Stroke* 34:2258–63

Koizumi J (1986) Experimental studies of ischemic brain edema: 1. A new experimental model of cerebral embolism in rats in which recirculation can be introduced in the ischemic area. *Jpn J Stroke* 8:1–8

Lee J, Elkahloun AG, Messina SA, Ferrari N, Xi D, Smith CL, Cooper Jr R, Albert PS, Fine HA (2003) Cellular and genetic characterization of human adult bone marrow-derived neural stem-like cells: a potential antiglioma cellular vector. *Cancer Res* 63:8877–89

Li Y, Chen J, Chen XG, Wang L, Gautam SC, Xu YX, Katakowski M, Zhang LJ, Lu M, Janakiraman N, Chopp M (2002) Human marrow stromal cell therapy for stroke in rat: neurotrophins and functional recovery. *Neurology* 59:514–23

Li Y, Chopp M, Chen J, Wang L, Gautam SC, Xu YX, Zhang Z (2000) Intrastriatal transplantation of bone marrow nonhematopoietic cells improves functional recovery after stroke in adult mice. *J Cereb Blood Flow Metab* 20:1311–9

Lin Y, Liu L, Li Z, Qiao J, Wu L, Tang W, Zheng X, Chen X, Yan Z, Tian W (2006) Pluripotency potential of human adipose-derived stem cells marked with exogenous green fluorescent protein. *Mol Cell Biochem* 291:1–10

Lindvall O, Kokaia Z (2006) Stem cells for the treatment of neurological disorders. *Nature* 441:1094–6

Loos M, Dihne M, Block F (2003) Tumor necrosis factor-alpha expression in areas of remote degeneration following middle cerebral artery occlusion of the rat. *Neuroscience* 122:373–80

Lu P, Blesch A, Tuszynski MH (2004) Induction of bone marrow stromal cells to neurons: differentiation, transdifferentiation, or artifact? *J Neurosci Res* 77:174–91

Lundkvist J, Lendahl U (2001) Notch and the birth of glial cells. *Trends Neurosci* 24:492–4

Mimura T, Dezawa M, Kanno H, Yamamoto I (2005) Behavioral and histological evaluation of a focal cerebral infarction rat model transplanted with neurons induced from bone marrow stromal cells. *J Neuropathol Exp Neurol* 64:1108–17

Morris R (1984) Developments of a water-maze procedure for studying spatial learning in the rat. *J Neurosci Methods* 11:47–60

Nguyen TH, Khakhoulina T, Simmons A, Morel P, Trono D (2005) A simple and highly effective method for the stable transduction of uncultured porcine hepatocytes using lentiviral vector. *Cell Transplant* 14:489–96

Ohta T, Kikuta K, Imamura H, Takagi Y, Nishimura M, Arakawa Y, Hashimoto N, Nozaki K (2006) Administration of ex vivo-expanded bone marrow-derived endothelial progenitor cells attenuates focal cerebral ischemia-reperfusion injury in rats. *Neurosurgery* 59:679–86; Discussion -86

Prockop DJ (1997) Marrow stromal cells as stem cells for nonhematopoietic tissues. *Science* 276:71–4

Puurunen K, Jolkkonen J, Sirvio J, Haapalinna A, Sivenius J (2001) Selegiline combined with enriched-environment housing attenuates spatial learning deficits following focal cerebral ischemia in rats. *Exp Neurol* 167: 348–55

Reubinoff BE, Itsykson P, Turetsky T, Pera MF, Reinhartz E, Itzik A, Ben-Hur T (2001) Neural progenitors from human embryonic stem cells. *Nat Biotechnol* 19:1134–40

Shen LH, Li Y, Chen J, Cui Y, Zhang C, Kapke A, Lu M, Savant-Bhonsale S, Chopp M (2007) One-year follow-up after bone marrow stromal cell treatment in middle-aged female rats with stroke. *Stroke* 38:2150–6

Shimizu S, Kitada M, Ishikawa H, Itokazu Y, Wakao S, Dezawa M (2007) Peripheral nerve regeneration by the in vitro differentiated-human bone marrow stromal cells with Schwann cell property. *Biochem Biophys Res Commun* 359:915–20

Takagi Y, Nishimura M, Morizane A, Takahashi J, Nozaki K, Hayashi J, Hashimoto N (2005) Survival and differentiation of neural progenitor cells derived from embryonic stem cells and transplanted into ischemic brain. *J Neurosurg* 103:304–10

Tang Y, Yasuhara T, Hara K, Matsukawa N, Maki M, Yu G, Xu L, Hess DC, Borlongan CV (2007) Transplantation of bone marrow-derived stem cells: a promising therapy for stroke. *Cell Transplant* 16:159–69

Veizovic T, Beech JS, Stroemer RP, Watson WP, Hodges H (2001) Resolution of stroke deficits following contralateral grafts of conditionally immortal neuroepithelial stem cells. *Stroke* 32:1012–9

Yanagisawa D, Qi M, Kim DH, Kitamura Y, Inden M, Tsuchiya D, Takata K, Taniguchi T, Yoshimoto K, Shimohama S, Akaike A, Sumi S, Inoue K (2006) Improvement of focal ischemia-induced rat dopaminergic dysfunction by striatal transplantation of mouse embryonic stem cells. *Neurosci Lett* 407:74–9

Yonemori F, Yamaguchi T, Yamada H, Tamura A (1999) Spatial cognitive performance after chronic focal cerebral ischemia in rats. *J Cereb Blood Flow Metab* 19:483–94

Supplementary Information accompanies the paper on the Journal of Cerebral Blood Flow & Metabolism website (http://www.nature.com/jcbfm)

Experimental Neurology xxx (2010) xxx–xxx

Contents lists available at ScienceDirect

Experimental Neurology

journal homepage: www.elsevier.com/locate/yexnr

Long-term observation of auto-cell transplantation in non-human primate reveals safety and efficiency of bone marrow stromal cell-derived Schwann cells in peripheral nerve regeneration

Shohei Wakao [a,1], Takuya Hayashi [b,1], Masaaki Kitada [a,1], Misaki Kohama [a], Dai Matsue [a], Noboru Teramoto [b], Takayuki Ose [b], Yutaka Itokazu [c], Kazuhiro Koshino [b], Hiroshi Watabe [b], Hidehiro Iida [b], Tomoaki Takamoto [d], Yasuhiko Tabata [d], Mari Dezawa [a,*]

[a] Department of Stem Cell Biology and Histology, Tohoku University Graduate School of Medicine, Sendai 980-8575, Japan
[b] Department of Investigative Radiology, Advanced Medical Engineering Center, National Cardiovascular Center Research Institute, Osaka 565-8565, Japan
[c] Department of Anatomy and Neurobiology, Kyoto University Graduate School of Medicine, Kyoto 606-8501, Japan
[d] Department of Biomaterials, Field of Tissue Engineering, Institute for Frontier Medical Sciences, Kyoto University, Kyoto 606-8507, Japan

ARTICLE INFO

Article history:
Received 19 November 2009
Revised 25 January 2010
Accepted 29 January 2010
Available online xxxx

Keywords:
Mesenchymal stem cells
Monkey
Schwann cells
Nerve regeneration
Peripheral nerve
Transdifferentiation

ABSTRACT

Based on their differentiation ability, bone marrow stromal cells (MSCs) are a good source for cell therapy. Using a cynomolgus monkey peripheral nervous system injury model, we examined the safety and efficacy of Schwann cells induced from MSCs as a source for auto-cell transplantation therapy in nerve injury. Serial treatment of monkey MSCs with reducing agents and cytokines induced their differentiation into cells with Schwann cell properties at a very high ratio. Expression of Schwann cell markers was confirmed by both immunocytochemistry and reverse transcription-polymerase chain reaction. Induced Schwann cells were used for auto-cell transplantation into the median nerve and followed-up for 1 year. No abnormalities were observed in general conditions. Ki67-immunostaining revealed no sign of massive proliferation inside the grafted tube. Furthermore, ^{18}F-fluorodeoxygluocose-positron emission tomography scanning demonstrated no abnormal accumulation of radioactivity except in regions with expected physiologic accumulation. Restoration of the transplanted nerve was corroborated by behavior analysis, electrophysiology and histological evaluation. Our results suggest that auto-cell transplantation therapy using MSC-derived Schwann cells is safe and effective for accelerating the regeneration of transected axons and for functional recovery of injured nerves. The practical advantages of MSCs are expected to make this system applicable for spinal cord injury and other neurotrauma or myelin disorders where the acceleration of regeneration is expected to enhance functional recovery.

Introduction

Schwann cells are peripheral glial cells that form the myelin of the peripheral nervous system (PNS) and have a major role in neuronal function including saltatory conduction. Following PNS injury, Schwann cells have a pivotal role in axonal degeneration and regeneration. During Wallerian degeneration, myelin is degraded and Schwann cells are activated and proliferate to produce a variety of neurotrophic factors, cytokines, and cell adhesion molecules, thereby providing a pathway for regenerating axons (Fawcett and Keynes, 1990; Hall, 2001; Radtke and Vogt, 2009; Torigoe et al., 1996). Schwann cells have a crucial role in the endogenous repair of the PNS by reconstructing myelin, which is indispensable for neurologic function. Schwann cells also support reconstruction of the injured central nervous system (CNS) where successful axonal regeneration and functional reconstruction are not normally achieved by oligodendrocytes (Dezawa and Adachi-Usami, 2000). Several experiments in the spinal cord and some other areas in the CNS have shown that the injection or transplantation of cultured Schwann cells induces axonal growth across the site of injury and contributes to functional recovery (Bunge, 2002; Bunge, 2008; Hill et al., 2006; Plant et al., 1998; Vukovic et al., 2007). For these reasons, Schwann cells have long attracted attention and are thus one of the most widely studied cell types for axonal regeneration both in the PNS and CNS.

Although Schwann cells have a strong ability to induce nerve regeneration, it is difficult to obtain a sufficient amount of Schwann cells for clinical use. Schwann cell cultivation requires another peripheral nerve being newly sacrificed. In addition, several technical

* Corresponding author. Department of Stem Cell Biology and Histology, Tohoku University Graduate School of Medicine, 2-1 Seiryo-machi, Aoba-ku, Sendai 980-8575, Japan. Fax: +81 22 717 8030.
E-mail address: mdezawa@m.tains.tohoku.ac.jp (M. Dezawa).
[1] These authors contributed equally.

0014-4886/$ – see front matter © 2010 Elsevier Inc. All rights reserved.
doi:10.1016/j.expneurol.2010.01.022

difficulties remain for harvesting and expanding a large number of Schwann cells. Accordingly, it is desirable to establish cells with Schwann cell characteristics from sources other than the PNS that are easy to access, capable of rapid expansion, amenable to survival, and able to integrate into the host tissue to elicit axonal regeneration and to contribute to re-myelination.

Therefore, we previously used bone marrow stromal cells (MSCs) as a source for inducing Schwann cells because MSCs are easily accessible through aspiration of the bone marrow from patients or a marrow bank and can be expanded in culture with fewer ethical problems compared to other sources. MSCs can be readily expanded in large scale for auto-transplantation, and have the potential to differentiate into other kinds of cells such as osteoblasts, adipocytes, and chondrocytes (Pittenger et al., 1999; Prockop, 1997).

Induction of Schwann cells from MSCs is efficiently achieved by first reverting human and rodent MSCs to an undifferentiated state using beta-mercaptoethanol (BME) followed by retinoic acid (RA) treatment and then inducing differentiation by treating them with forskolin (FSK), basic fibroblast growth factor (bFGF), platelet-derived growth factor (PDGF), and neuregulin, all of which are factors related to Schwann cell differentiation (Dezawa et al., 2001). The induced cells are different from the original untreated MSCs, but are morphologically quite similar to Schwann cells and express Schwann cell markers at a high ratio (Dezawa et al., 2001). The effectiveness of this induction system was also demonstrated by other groups in other mesenchymal stem cells such as adipose-derived stem cells (Jiang et al., 2008; Kingham et al., 2007; Xu et al., 2008).

It is noteworthy that human and rodent MSC-derived Schwann cells express myelin-related markers and contribute to re-myelination when transplanted into rat sciatic nerve injury (Mimura et al., 2004; Shimizu et al., 2007), and also effectively promote axonal regeneration and functional recovery in spinal cord injury (Kamada et al., 2005; Someya et al., 2008). These findings demonstrate that MSC-derived Schwann cells are effective for both PNS and CNS regeneration.

To extend this system to clinical application, the safety and effectiveness in higher mammals must be evaluated. The potential for auto-cell transplantation is one of the strong advantages of MSCs. In this study, we estimated the safety and effectiveness of MSC-derived Schwann cells for auto-cell transplantation in a PNS injury model in cynomolgus monkey. The expression of Schwann cell markers in the MSC-derived Schwann cells was confirmed by both immunocytochemistry and reverse transcription-polymerase chain reaction (RT-PCR). Artificial grafts were made by transferring MSC-derived Schwann cells into trans-permeable tubes filled with 3-dimensional collagen, transplanted into the gap between transected median nerve segments, and followed-up for 1 year. No abnormalities were observed in general conditions. In ^{18}F-fluorodeoxygluocose (FDG)-positron emission tomography (PET) scanning, which allows for highly sensitive detection of neoplastic cells, no abnormal accumulation of radioactivity was observed except in regions known to have physiologic accumulations. Cell proliferation assessed by Ki67 immunostaining demonstrated no mass formation and low proliferation of cells. Restoration of the transplanted nerve was confirmed by the hand movement analysis, electrophysiology, and histology.

These results suggest that auto-cell transplantation therapy using MSC-derived Schwann cells is effective and is very likely to be safe for nerve injury. The practical advantages of MSCs is expected to make this system applicable for treatment of spinal cord injury and other neurotrauma or neurodegenerative diseases where Schwann cell transplantation is expected to be effective.

Materials and methods

Animal experiments using cynomolgus monkeys were approved by the Animal Care and Experimentation Committee of the Kyoto University Graduate School of Medicine, Tohoku University Graduate School of Medicine and the National Cardiovascular Center Research Institute. Six adult male cynomolgus monkeys (3 to 4 years of age) were used in this experiment. Cynomolgus monkeys have been broadly used to evaluate the efficiency of transplantation methods particularly in PNS injury models (Ahmed et al., 1999; Archibald et al., 1995; Auba et al., 2006; Hess et al., 2007; Lee et al., 2008). Furthermore, we have previously confirmed the transdifferentiation capacity of MSCs in cynomolgus monkeys, i.e., to be induced into neuronal cells (Nagane et al., 2009). For these reasons, we chose cynomolgus monkeys as the experimental animal in this study.

Isolation of monkey MSCs and Schwann cell induction

Primary monkey MSCs were isolated from the pelvic bone. Bone marrow aspirate (5 ml) was diluted 1:10 using culture medium comprised of alpha-minimum essential medium (MEM), 15% fetal bovine serum (FBS), 2 mM L-glutamine, and kanamycin and incubated at 37 °C, 5% CO_2. After 4 days, non-adherent cells were removed by replacing the medium. Adherent MSCs were expanded when they reached 95% confluence, and were subcultured 4 times, and then finally subjected to the Schwann cell induction.

MSCs were subcultured at a density of 1.76×10^3 cells/cm^2 and incubated in alpha-MEM containing 1 mM BME without serum for 24 h. The culture medium was then replaced with alpha-MEM containing 10% FBS and 35 ng/ml all-trans-RA (Sigma, St. Louis, MO). Three days later, cells were transferred to alpha-MEM containing 10% FBS, 5 μM FSK (Calbiochem, La Jolla, CA), 10 ng/ml bFGF (Peprotech, London, UK), 5 ng/ml PDFG-AA (Peprotech, London, UK), and 200 ng/ml heregulin-ß1-EGF-domain (R&D Systems, Minneapolis, MN) and cultured for 4 to 5 days. These Schwann cells induced from MSCs were called 'M-Schwann cells' in the following sections.

Evaluation of M-Schwann cells

M-Schwann cells were evaluated using both phase-contrast microscopic observation and immunocytochemistry. For immunocytochemistry, the YST-1 cell line was used for positive control (RIKEN, Ibaraki, Japan), monkey naïve MSCs as a negative control, and monkey M-Schwann cells were fixed with 4% paraformaldehyde in 0.02 M phosphate buffered saline (PBS). Primary antibodies used for the immunocytochemistry were anti-protein zero (P0) rabbit IgG (1:300, kindly provided by Dr. J.J. Archelos, Karl-Franzens Universitat, Graz, Austria), anti-p75 (nerve growth factor receptor) mouse IgG (1:500, Abcam Cambridge, UK), anti-glial fibrillary acidic protein (GFAP) rabbit IgG (1:300, DAKO, Carpinteria, CA), anti-O4 mouse IgM (1:20, Boehringer Ingelheim GmbH, Ingelheim, Germany), anti-CD90 mouse IgG (1:400, BD Bioscience, Bedford, MA), and anti-smooth muscle actin (SMA) mouse IgG (1:400, LabVision, Newmarket, Suffolk, UK). These primary antibodies were detected by Alexa 568-conjugated anti-rabbit IgG, anti-mouse IgG, or anti-mouse IgM antibodies (Molecular Probes, Invitrogen, Carlsbad, CA). Immunocytochemistry was performed as previously described (Kitada et al., 2001). Briefly, samples were incubated in 20% BlockAce (skim milk, Yukijirushi, Tokyo, Japan) in 0.005% saponin and 50 mM glycine in PBS (SaGlyPBS) for 10 min, incubated with the primary antibody in 5% BlockAce in SaGlyPBS overnight at 4 °C followed by the secondary antibody incubation in 5% BlockAce in SaGlyPBS. Nuclei were counterstained with 4′, 6-diamidino-2-phenylindole (DAPI, Molecular Probes). As for immunostaining against CD90, cells were incubated with anti-CD90 antibody in culture medium at 37 °C, 5% CO_2, washed, fixed with 4% paraformaldehyde in 0.02 M PBS, and further processed for secondary antibody incubation. All images were taken by a confocal laser scanning microscope (CS-1, Nikon, Kawasaki, Japan) with the same laser intensity and detection sensitivity.

Please cite this article as: Wakao, S., et al., Long-term observation of auto-cell transplantation in non-human primate reveals safety and efficiency of bone marrow stromal cell-derived Schwann..., Exp. Neurol. (2010), doi:10.1016/j.expneurol.2010.01.022

Expression of Schwann cell markers in RT-PCR

Total RNA from naïve MSCs and M-Schwann cells was extracted using an RNeasy Mini Kit (Qiagen GmbH, Hilden, Germany) and purified in accordance with the manufacturer's instructions. From 1 μg of total RNA, first-strand cDNA was generated using SuperScript II reverse transcriptase (Invitrogen, Carlsbad, CA). The PCR reactions were performed using Ex Taq DNA polymerase (TaKaRa, Tokyo, Japan). The amplification conditions were: 1 min at 94 °C, 1 min at 60 °C, and 1 min at 72 °C, for 30 cycles (25 cycles for β-actin) and a final incubation at 72 °C for an additional 7 min.

We used the following *Macaca fascicularis* PCR Primers that are specific genes for Schwann cells, and β-actin as internal control. ß-actin sense: 5′-TCTAGGCGGACTGTGACTTAGTTGCGTTAC-3′ and antisense: 5′-AATCAAAGTCCTCGGCCACATTGTAGAACT-3′, GFAP sense: 5′-TGCCCTAGGCTCCATCAGTATT-3′ and antisense: 5′-TCCCAGATACC-CTGAGAGAACCT-3′, Krox20 sense: 5′-AGTACCCCAACAGACCTAG-CAAGA-3′ and antisense: 5′-GCAAACTTTCGGCCACAGTAG-3′, MBP sense: 5′-CCCACACACCCCAATTAGCT-3′ and antisense: 5′-GCATCAC-GCTGACTACTCCTCAT-3′.

M-Schwann cell autologous PNS graft

The composition and construction of the biodegradable conduit and collagen sponge were previously reported (Hisasue et al., 2005). Briefly, the copolymer was composed of 75% L-lactic acid and 25% E-caprolactone. A rotating polytetrafluoroethylene tube 2 mm in diameter was dipped in the copolymer solution, immersed in liquid nitrogen for a few minutes, and air dried at 25 °C for 24 h. The tube used for transplantation was 4 mm long with 2-mm internal and 3-mm external diameters. A solid sample of atelocollagen (Nippon Meat Packers, Osaka, Japan; 70 wt.% type I and 30 wt.% type III collagen) was used for sponge preparation. Atelocollagen was dissolved in HCl aqueous solution to a final concentration of 1.0 wt.%. The collagen solution was whipped on a homogenizer, frozen at −80 °C, and freeze-dried. Collagen sponge was prepared by cutting it into pieces to fill the biodegradable conduit. The fabricated guide tubes and collagen sponge were sterilized with ethylene oxide gas before use. This artificial conduit can hold cells or tissue, which will be a scaffold for supporting axonal regeneration. Also, this artificial conduit is gas permeable so that cells inside the graft are able to survive after transplantation (Mligiliche et al., 2003).

To determine the cell concentration of the artificial grafts, we inspected normal monkey median nerve sections by Giemsa staining. We calculated 250 myelinated axons were contained within an area of 110 μm^2, suggesting 250 Schwann cells are myelinating axons in this square measure. The total transverse area of the monkey median nerve, except for the epineurium, was approximately 1570 μm^2. Based on the average length of a Ranvier's node (~1000 μm), a 1-cm nerve segment is estimated to contain approximately 2×10^6 Schwann cells. Thus, the tube was filled with induced M-Schwann cells at a concentration of 2×10^6 cells suspended in 30-μl 0.01 M PBS per 1-cm tube and incubated in 10% FBS containing alpha-MEM for several hours in 5% CO2 at 37 °C before transplantation. The graft was longitudinally cut and counterstained with Hoechst 33342 to observe the distribution of the cells inside the graft.

Transplantation of autologous M-Schwann cell grafts to median nerve

We chose the median nerve to make the PNS injury model, because this nerve is relatively easily accessible and the function of this nerve is easier to evaluate during the regenerative period, rather than any other nerves in cynomolgus monkey (Archibald et al., 1995). Just before transplantation, the motor nerve conduction study (described below) was performed under ketamine- and xylazine-induced general anesthesia. A 20-mm segment of unilateral median nerve was completely removed 2 cm proximal to the wrist joint of the forearm and the artificial graft was anastomosed to the proximal and distal nerve tips and their neurilemma using 10-0 nylon sutures at both ends. Five monkeys (M-Schwann cell-transplanted group) received auto-cell transplantation of the M-Schwann cells, while two monkeys (the sham-operated group) received transplantation of empty artificial grafts that were not filled with M-Schwann cells. Just after transplantation, a motor nerve conduction study performed again to confirm the absence of CMAP indicated that the median nerve was completely transected. For auto-cell transplantation, M-Schwann cells were all derived from each recipient animal so that no immunosuppression was given after transplantation.

General health and behavior analyses

Weight check and blood tests (urea nitrogen, creatinine, creatine phosphokinase, aspartate amino transferase, alanine transferase, lactate dehydrogenase, platelet, hemoglobin, red blood cells, white blood cells, hematocrit, mean corpuscular volume, mean corpuscular hemoglobin, mean corpuscular hemoglobin concentration, D-dimer and fibrinogen A) were performed every month before and after transplantation.

For behavioral analysis, movements of the hand and thumb, and grip strength for obtaining food of both the transplanted and intact sides were recorded on a video tape and analyzed for evaluation. The criteria for hand motion and functional recovery scores were as follows:

Score 5: Strength of the thumb, hand movement, and frequency of hand use for feeding and general behavior, such as grabbing the cage, are nearly equal between operated and intact sides.

Score 4: Strength of the thumb is asymmetrical, but the frequency of the use of the hands is nearly the same in both sides. Monkey is able to grab, but is unable to pinch small objects less than 1 cm.

Score 3: Monkey can grab the cage, but muscular force of the operated hand is weak. The thumb is contractured. Wrist movement compensates for the weakness of the hand and thumb. The muscle force of the thumb is less than half that of the intact side.

Score 2: Functional recovery is weak. Movement of the thumb is observed, but compensation by the wrist is recognized. The use of the operated hand during feeding is rare.

Score 1: Little hand and finger motion on the operated side. Monkey is unable to grab objects.

Score A: Unmeasurable. Monkey is unable to make contact because of too much guarding.

The evaluation was conducted by a person, who did not operate animals, without any information about the animal including the procedure of transplantation, and the observation period after the transplantation.

Motor nerve conduction study

To estimate the restoration of nerve function, we performed motor nerve conduction study at five time points for each animal, just before and after transplantation and at 3, 6, and 12 months after the transplantation. To record the compound muscle action potential (CMAP) in the motor nerve conduction study, we pasted the anode electrode plate on the skin of the palmar side at the proximal joint of the first digit, the cathode electrode plate on the belly muscle of the abductor pollicis brevis, and the ground plate on the back of the forearm (Someya et al., 2008). The median nerve was stimulated with a rectangular wave-shaped pulse using a bipolar stimulator by placing its cathode at either of the following sites; 5-cm proximal to the wrist joint (3 cm proximal to the transplanted site) and at the cubital fossa. At each stimulation site, we applied electrical current of supramaximal intensity (varying from 5 mA to 25 mA) within a range that did not induce ulnar nerve stimulation. For each study, we recorded the CMAP, distal latency (time latency between the stimulus

Please cite this article as: Wakao, S., et al., Long-term observation of auto-cell transplantation in non-human primate reveals safety and efficiency of bone marrow stromal cell-derived Schwann..., Exp. Neurol. (2010), doi:10.1016/j.expneurol.2010.01.022